

Search for dark matter production in association with top quarks in the dilepton final state at $\sqrt{s} = 13$ TeV

Pablo Martínez Ruíz del Árbol, Jónatan Piedra Gomez, Cédric Prieëls
February 4th 2022

Thesis Endorsement
Instituto de Física de Cantabria

Introduction

A search for the production of dark matter particles in association with either one or two top quarks is presented:

- We study the pp collisions produced by the LHC at $\sqrt{s} = 13$ TeV;
- Data collected by the CMS detector;
- Legacy analysis, considering the full Run II dataset (data collected in 2016, 2017 and 2018 and summing around 137 fb^{-1}).

Motivation

- Several (mostly astrophysical) evidences for the existence of dark matter, however **its nature remains unknown** and it has never been detected experimentally;
- If dark matter is made of some kind of particle it might be produced in the high energy collisions.

Main objective

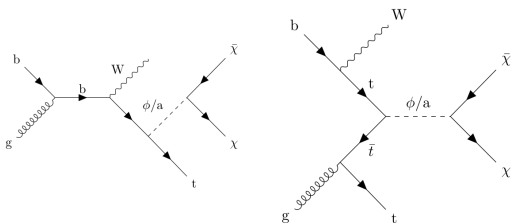
- Consider different dark matter production models to discover or eventually exclude some of them, or **put upper limits on their cross section of production**.

Work done and previous results

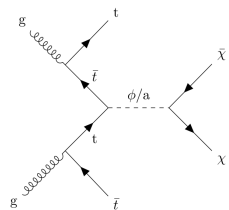
We are searching for **dark matter produced in association with either one or two top quarks**. Several **simplified models** are interesting to consider:

- Spin 1/2 DM χ ($\in [1, 55]$ GeV, Dirac fermion)
- Spin 0 scalar (S)/pseudoscalar (PS) mediator ϕ/a (Yukawa-like structure of such interactions → gain from the coupling of the mediator to top quarks)
- Mediator mass $\in [10, 1000]$ GeV
- Coupling g_χ mediator/DM set to 1 (same for all g_q couplings)

t/\bar{t} +DM tW models



$t\bar{t}$ +DM model



The **typical final state** of such models is made out of:

- 1 or 2 b-tagged jets coming from the decay of the top quark(s);
- 2 W bosons, seen as a combination of jets and leptons depending on the channel;
- Some MET coming from the dark matter and the decay of the Ws;

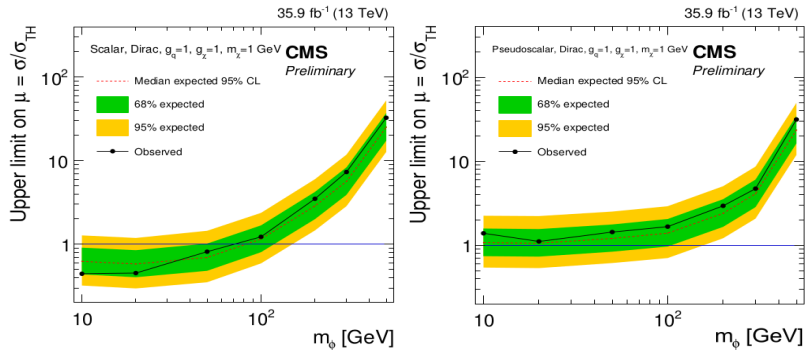
In particular, we are studying the **dilepton final state** in this work:

- Has the lowest branching ratio: $\text{BR}(W \rightarrow l^+ + \nu_l) = (10.80 \pm 0.09)\%$ for each of the tree leptons (contains only 5% of the signal events);
- But, leptons can usually be reconstructed better than jets, resulting in lower systematic uncertainties;
- And this channel also has the lowest number of backgrounds, resulting in a better signal isolation.

This channel is then **expected to be competitive with the hadronic channel**, especially when considering high mediator masses, which feature a higher global signal/background discrimination.

Previous relevant results I

A similar analysis has already been carried out by CMS using 2016 data, considering the $t\bar{t}$ +DM signal only and the dilepton final state only (AN-2016-478).



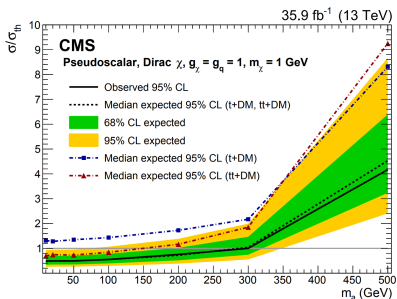
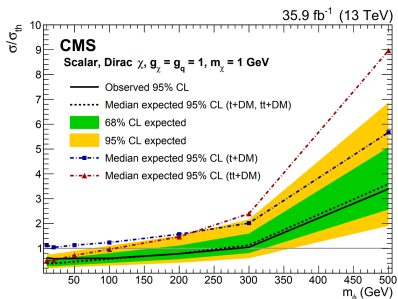
The observed (expected) limits excluded a scalar mediator with mass below 80 (70) GeV, while no exclusion was achieved when considering pseudoscalar mediators.

Previous relevant results II

A combination of both the $t/\bar{t}+DM$ and $t\bar{t}+DM$ processes has also been performed.

The inclusion of the single top signal process improved up to a factor 2 the limits obtained by the $t\bar{t}$ analysis on its own. This analysis:

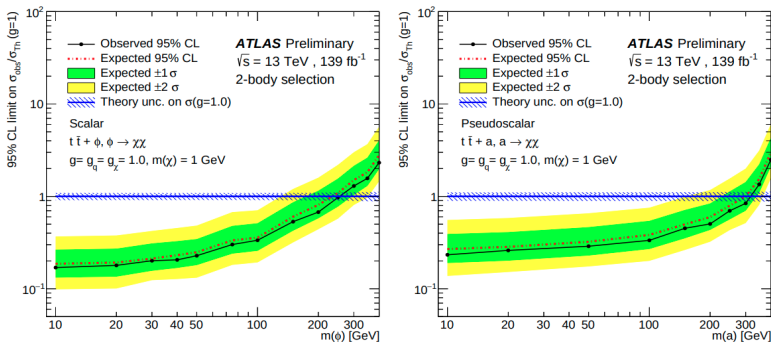
- Only considered the 2016 data-taking period;
- And only considered the semi-leptonic and hadronic final states.



Scalar (pseudoscalar) mediators were with this combination excluded up to 290 (300) GeV at the 95% confidence level.

Previous relevant results III

The ATLAS collaboration also obtained the exclusion limits obtained using the full Run II legacy dataset and considering the dilepton final state only (ATLAS-CONF-2020-046).



They obtained expected scalar (pseudoscalar) exclusion limits of 250 (300) GeV, even though they used NLO cross-sections for the signals, around 30% higher than ours.

Global strategy

Analysis strategy

Run II legacy paper being worked on, expected to combine both the $t/\bar{t}+DM$ and $t\bar{t}+DM$ searches, and the 3 possible final states (hadronic, semi-leptonic and dileptonic).
→ Pre-approval process expected to start within a few weeks.

The effort is **globally common** between the groups studying the different final states:

- Objects are defined in a common way;
- Control and signal region orthogonal between the channels.
 - Number of leptons and b-jet categorization to improve the sensitivity by defining enriched $t/\bar{t}+DM/t\bar{t}+DM$ regions.

This talk will be focused on the **dilepton final state**, in which we are mostly involved, along with a team of DESY. Deborah Pinna and her team from the University of Wisconsin are focused on the semi-leptonic and hadronic channels.

Given that my PhD thesis is now coming to an end, with no further extensions possible, I would like to ask the conveners to endorse the results presented next and also fully documented in the AN-2022-014.

Samples and objects

Data

Single/double leptons datasets built to avoid any eventual double counting, considering the 3 years of the Run II of operation of the LHC:

- $(35.9 \pm 0.9) \text{ fb}^{-1}$
- $(41.5 \pm 1.0) \text{ fb}^{-1}$
- $(59.7 \pm 1.5) \text{ fb}^{-1}$

A blinding policy was followed at first, allowing us to only look at 1 fb^{-1} of data per year near the signal regions.

Monte-Carlo

The major backgrounds have been considered from MC and read from NanoAOD. Each year has its corresponding MC samples:

- $t\bar{t}$: decaying to both 1 and 2 leptons;
- Single top: s, t and tW channels considered;
- Drell-Yan: HT-binned samples to increase the statistics, with a correction factor derived from data applied;
- TTZ and TTW: usually grouped together as TTV, and considering both the hadronic and leptonic final states;
- Others, such dibosons and tribosons production, all taken from MC.

Signal samples

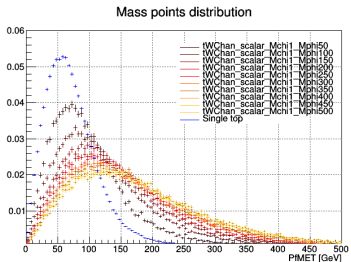
Both signal samples have been generated using MADGRAPH and PYTHIA8 (with the CP5 tune) at LO, while simulated events are then interfaced with a realistic model of the CMS detector using Geant4 [113] and are reconstructed using the official CMS reconstruction algorithms.

The $t/\bar{t}+DM$ process was **produced privately** (central request has been made but not yet processed), while the $t\bar{t}+DM$ was **generated centrally**. In both cases:

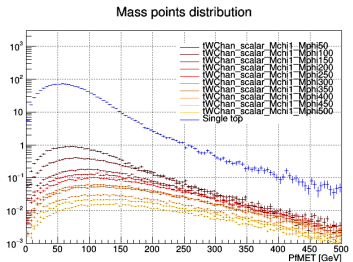
- Both scalar and pseudoscalar mediators are considered;
- 400.000 events were produced for each mediator mass, from 10 to 1000 GeV;
- The dark matter mass was set to 1 GeV, but additional samples ranging from 1 to 55 GeV were also produced;
- All the g_q and g_χ couplings were set to 1.

Scalar mediators

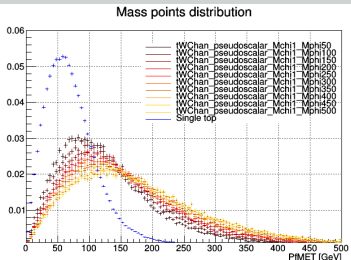
With normalization



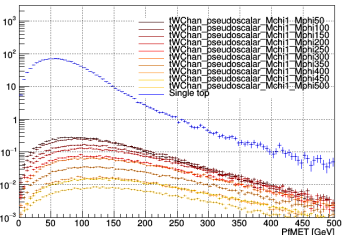
Without normalization



Pseudoscalar mediators

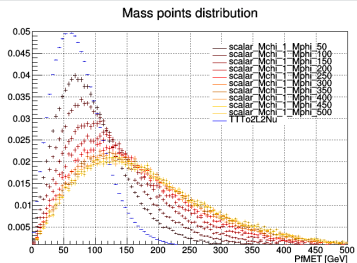


Mass points distribution

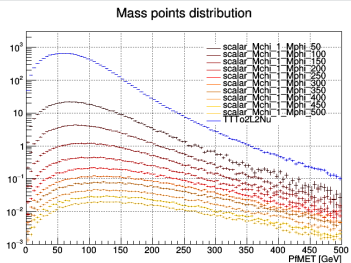


Scalar mediators

With normalization

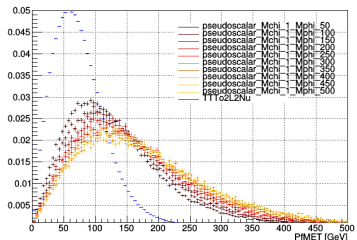


Without normalization

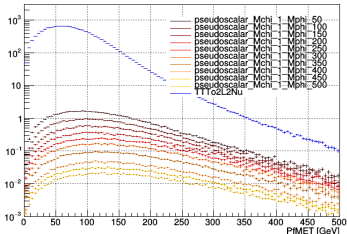


Pseudoscalar mediators

Mass points distribution



Mass points distribution



Objects definition I

We are currently using the following objects:

Triggers

- Single and double lepton triggers combined to gain statistics;
- Any possible double counting of events in multiple trigger is taken care of;
- Trigger p_T carefully chosen to avoid any turn-on effect;
- SingleMuon, SingleEle, DoubleMuon, DoubleEG, MuonEG (2016) and SingleMuon, EGamma, DoubleMuon, MuonEG (2017/2018) data streams considered;
- All the triggers used are listed in the backup.

Leptons

- Analysis relies on the selection of events with two leptons, with a leading (trailing) $p_T > 25(20)$ GeV and $|\eta| < 2.4$;
- Medium cut based POG WP used for electrons without additional ISO cut;
- Medium cut based POG WP for muons with tight ISO ($\text{pfRelIso04_all} < 0.15$);
- Additional small cuts on the impact parameters to reduce the non-prompt contamination in the MET tail ($|d_0| < 0.05$ cm, $|d_z| < 0.1$ cm, $S_{3D}^d < 4$).

Jets

- Clustered from the PF candidates using the **anti-kT algorithm**;
- Basic selection: $p_T > 30 \text{ GeV}$, $|\eta| < 2.4$;
- **Tight JET/MET POG** working point (efficiency and background rejection $> 98\%$), tight jet PU ID applied to jets with $p_T < 50 \text{ GeV}$ to reject PU jets contamination;
- $\Delta R > 0.4$ away from any lepton passing the criteria established for analysis to prevent signal leptons clustered as jets from entering the jet counting.

B-tag

- B-Tagging and Vertexing POG **deep CSV b-tag medium working point** (high efficiency, misidentification rate for a light jet as a b-jet $\sim 10\%$);
- B-tagging weight larger than 0.6321, 0.4941 or 0.4184 (2016, 2017 or 2018).

MET

- **PfType1MET** considered by propagating the JECs to the MET;
- All recommended **MET filters applied** to filter anomalous high MET events due to several detector issues, such as eventual dead cells in the calorimeters;
- XY-shift (ϕ modulation fix) and EE noise (2017) corrections applied on top.

Event selection

Minimal event selection

We require for the analysis:

- Leading (trailing) opposite sign lepton $p_T > 25$ (20) GeV;
- Third lepton veto ($p_T < 10$ GeV);
- $m_{\parallel} > 20$ GeV to avoid low mass resonances;
- At least 1 jet.

Pre-selection region

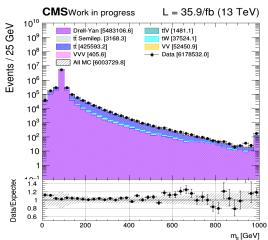
A pre-selection region is then defined by asking for:

- At least 1 medium deep CSV b-jet;
- A 15 GeV Z-veto on the ee and $\mu\mu$ channels;
- $\text{MET} > 100$ GeV and $M_{T2}^{\parallel} > 80$ GeV to keep this region orthogonal to the $t\bar{t}$ control regions used by the semi-leptonic channel.

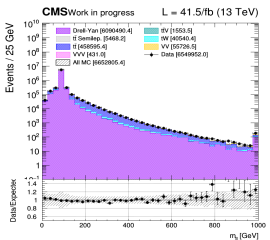
This region is used as the basis for the definition of our signals regions.

Minimal event selection region

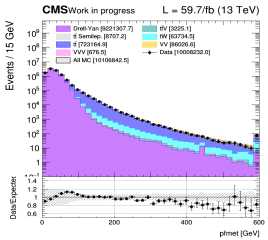
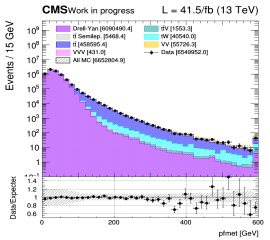
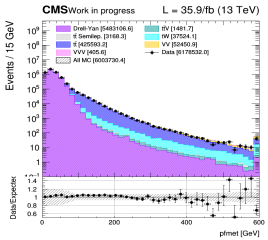
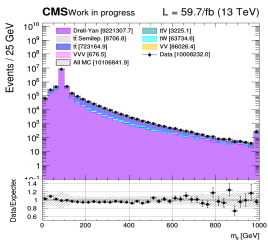
2016



2017

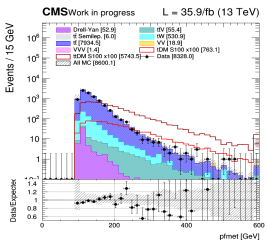


2018

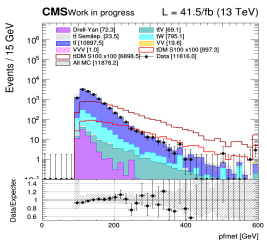


Pre-selection region

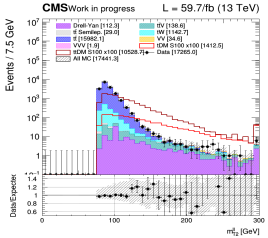
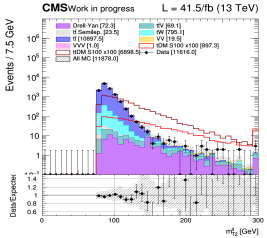
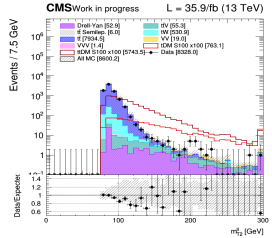
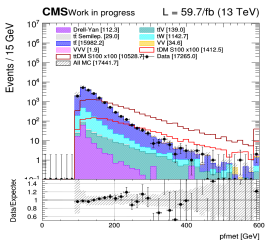
2016



2017



2018



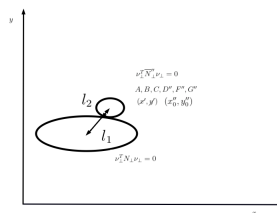
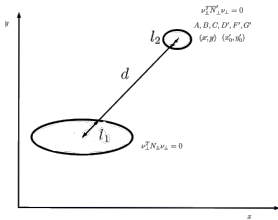
Signal extraction

Top reconstruction I

Many discriminating variables for our signals require knowledge of the top quark and anti-quark 4-momenta, only available after a **complete reconstruction of the $t\bar{t}$ system**.

The **Batchchart analytical method** was used, relying on a geometrical approach to analytically solve equations constraining the decay of top quarks involving leptons:

- Invariant mass constraints from the top quark and W boson imply that the solution set for each neutrino 4-momentum can be constrained to an ellipse;
- A typical SM $t\bar{t}$ event will give two ellipses close to each other, while ellipses coming from a typical signal event will be further apart and will not intersect.



Two discriminating variables naturally arise from this reconstruction: the **dark p_T** , defined as the distance between the centroids of the ellipses, and the **overlapping factor R** , defined as the ratio between the size of the ellipses and the distance between them.

In practice, **several complications** were taken into account:

- 0, 2 or 4 intersections can be observed while only 1 is physical, considered to be the solution with the lowest possible invariant mass for the $t\bar{t}$ system;
- All the leptons and (b-)jets combinations of the event were taken into account;
- A **smearing process** was followed to evaluate the impact that imperfectly measured kinematic variables can have on this process (100 iterations per event, by updating several parameters such as the energy/direction of the jets and leptons within their uncertainties).

These considerations allowed to **increase the mean top reconstruction efficiency from around 70 to 90%**. Non-physical default values are set to all the variables which depend on the value of the neutrino momenta for the events which still fail this reconstruction.

We trained both a BDT and an ANN, featuring the following common characteristics:

- Mix of standard model $t\bar{t}$ and single top as **backgrounds**, and mix of both $t/\bar{t}+DM$ and $t\bar{t}+DM$ as **signals**;
- Only events passing the **pre-selection cuts** are considered for the training;
- One specific training performed per signal mass point, and per signal region:
 - One targeting the $t/\bar{t}+DM$ signal, by considering events having exactly 1 jet, or exactly 2 jets and 1 b-jet;
 - Another one targeting the $t\bar{t}+DM$ signal, by considering events having exactly 2 jets and more than 1 b-jet, or more than 2 jets.
- 70%/30% train/test splitting used (~ 50.000 training events in total);
- 14 different discriminating variables used as input, all documented in the backup.

At the end of the day though, the **BDT was chosen for the analysis** over the ANN, given that it gave $\sim 10\%$ better upper limits once optimized. The BDT output shape is then used to perform a general **shape analysis**.

Hyperparameters optimization

The hyperparameters of the BDT have been fully optimized one by one, trying each time to minimize the error in the test dataset and the discrimination obtained.

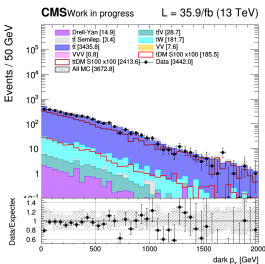
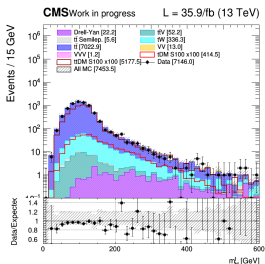
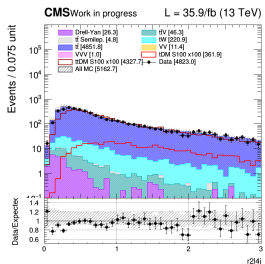
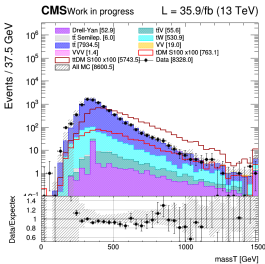
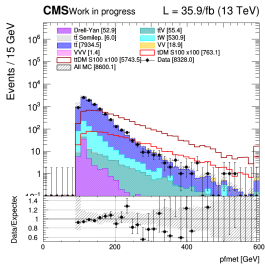
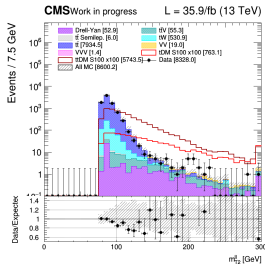
| DNN parameter | Optimized value |
|------------------------------|------------------|
| Maximum depth | 4 |
| Minimum samples per leaf | 2% |
| Loss function | Quadratic |
| Boost algorithm | Gradient descent |
| Shrinkage | 0.3 |
| Grid points n_{cut} | 1000 |
| Number of trees | 250 |

The following variables were observed to have the most impact on the final results:

| Rank | $t/\bar{t} + \text{DM}$ region | | $t\bar{t} + \text{DM}$ region | |
|------|--------------------------------|----------------------|-------------------------------|----------------------|
| | Variable | Importance | Variable | Importance |
| 1 | M_{T2}^{II} | $4.17 \cdot 10^{-1}$ | M_{T2}^{II} | $3.92 \cdot 10^{-1}$ |
| 2 | E_T^{miss} | $3.41 \cdot 10^{-1}$ | E_T^{miss} | $3.14 \cdot 10^{-1}$ |
| 3 | mass T | $1.28 \cdot 10^{-1}$ | mass T | $2.28 \cdot 10^{-1}$ |
| 4 | $r2l4j$ | $1.14 \cdot 10^{-1}$ | $r2l4j$ | $1.91 \cdot 10^{-1}$ |
| 5 | m_{bl}^t | $6.12 \cdot 10^{-2}$ | m_{bl}^t | $9.35 \cdot 10^{-2}$ |
| 6 | Dark p_T | $1.59 \cdot 10^{-2}$ | nbJet | $1.69 \cdot 10^{-2}$ |

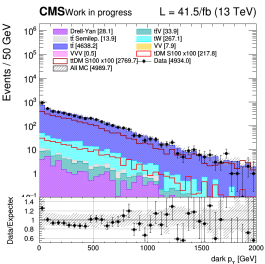
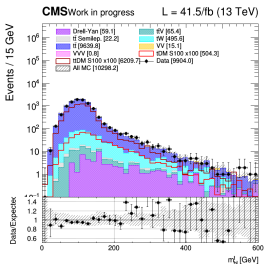
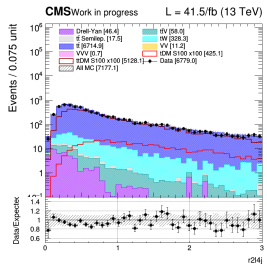
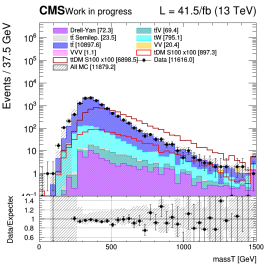
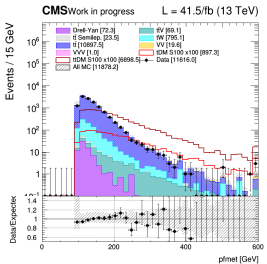
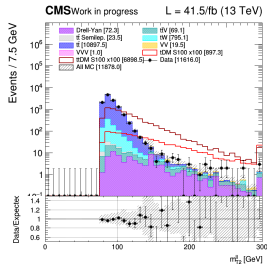
Discriminating variables

2016



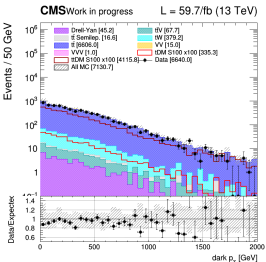
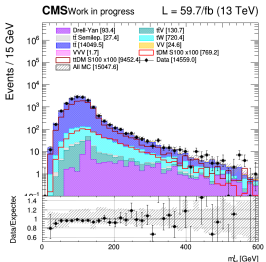
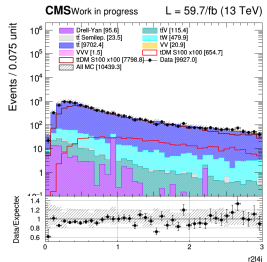
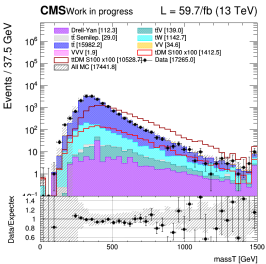
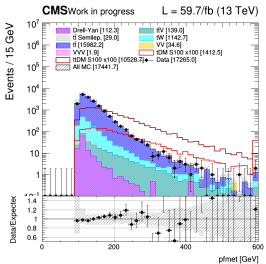
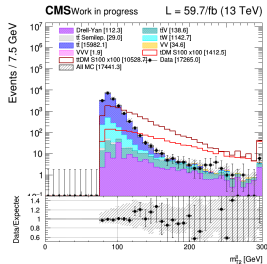
Discriminating variables

2017



Discriminating variables

2018

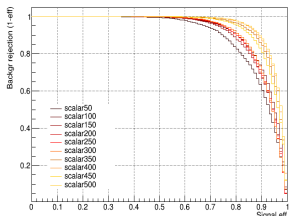


ROC curves

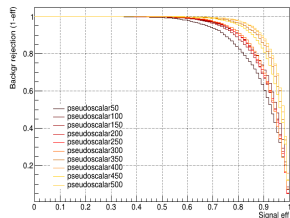
ROC curves have been obtained for all the different mass points available, from 50 to 500 GeV, for both scalar and pseudoscalar mediators, in both signal regions.

$t/\bar{t}+DM$ region

ROC curves for several trainings

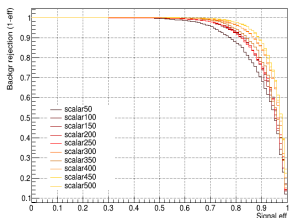


ROC curves for several trainings

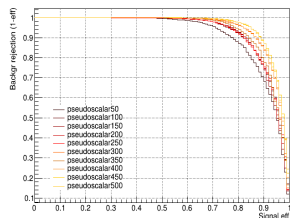


$t\bar{t}+DM$ region

ROC curves for several trainings



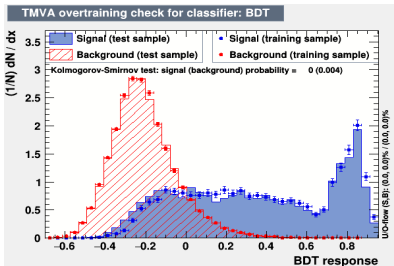
ROC curves for several trainings



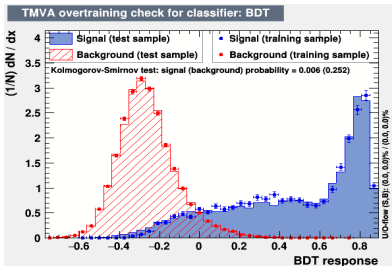
Overtraining check (t/\bar{t} +DM region)

Scalar mediators

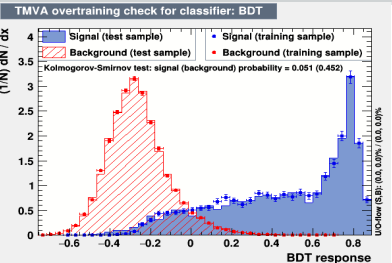
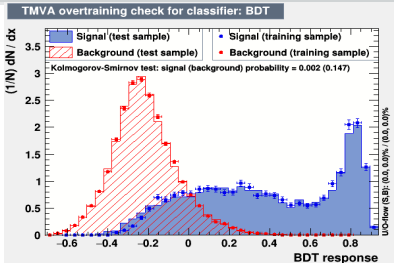
100 GeV



500 GeV



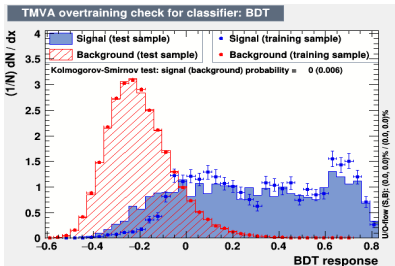
Pseudoscalar mediators



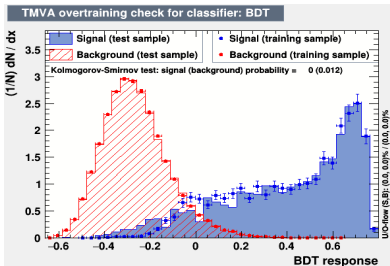
Overtraining check ($t\bar{t}$ +DM region)

Scalar mediators

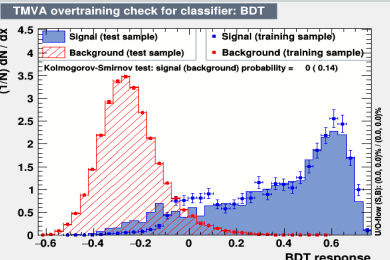
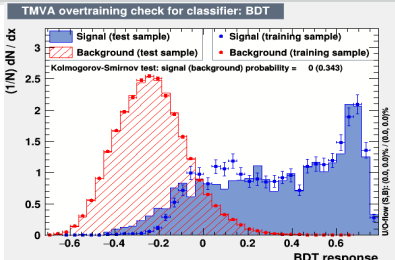
100 GeV



500 GeV



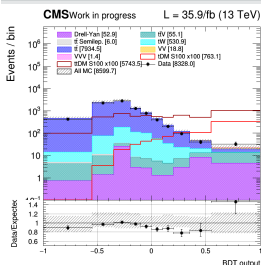
Pseudoscalar mediators



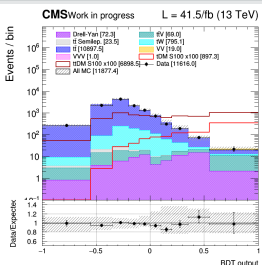
BDT scalar 100 GeV output shape

t/\bar{t} +DM region

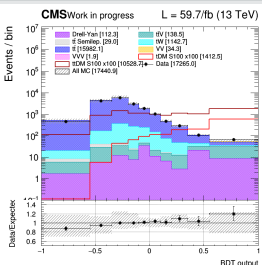
2016



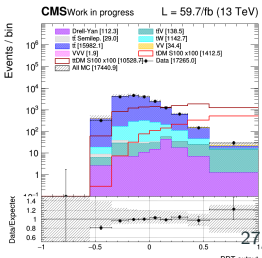
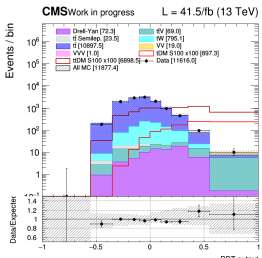
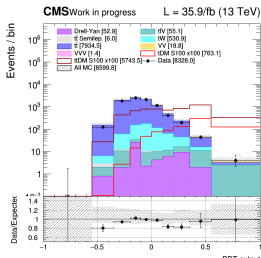
2017



2018



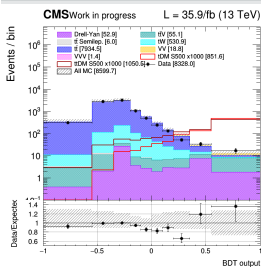
$t\bar{t}$ +DM region



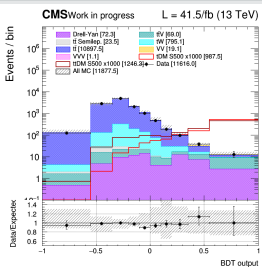
BDT scalar 500 GeV output shape

t/\bar{t} +DM region

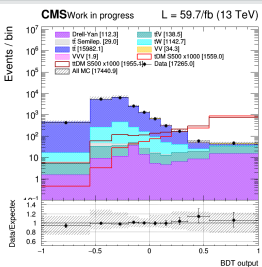
2016



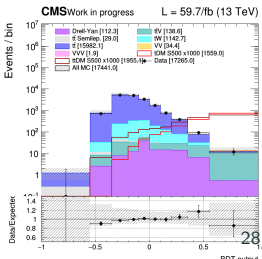
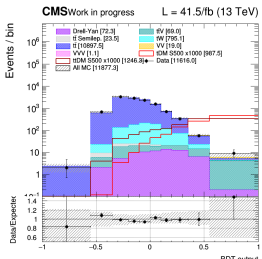
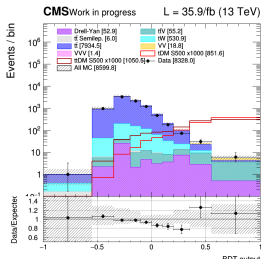
2017



2018



$t\bar{t}$ +DM region



Background prediction methods

Main background processes

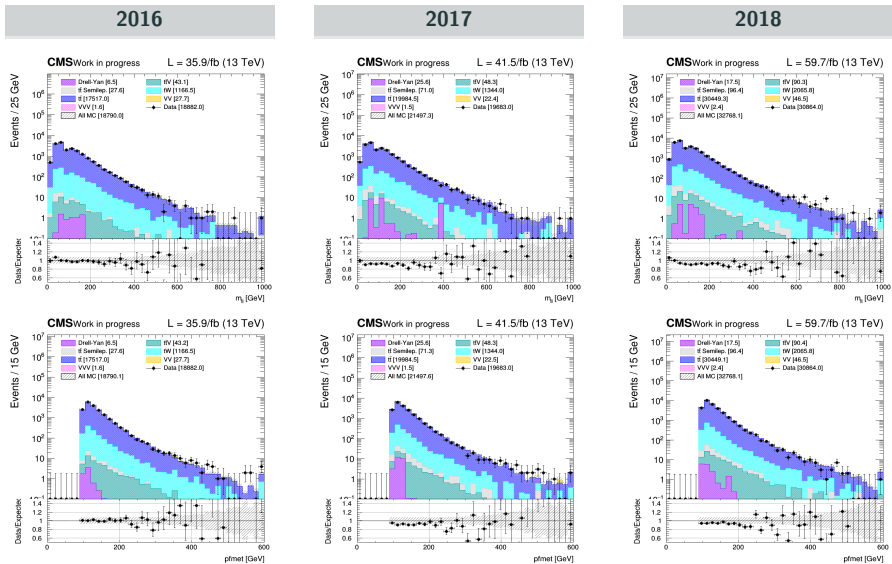
The backgrounds are predicted either directly from Monte-Carlo simulations or from semi data-driven methods.

- The **$t\bar{t}$ and the single top** are taken from simulation accounting for all the variations in the generation parameters. Several parameters (QCD scale, PDF variation,...) are varied and included as a systematic (see later) → a data validation region (low $M_{T_2}^H$) is explored to ensure the quality of the prediction;
- The **Drell-Yan** yields are obtained from a semi data-driven method using the excluded same flavor region on the Z peak as control region;
- **ttV, diboson, triboson processes and other minor backgrounds** are taken directly from MC simulations.

Recommended correction factors (L1 ECAL prefiring in 2016 and 2017, HEM issue in 2018) are then applied to the simulation.

Top control region

Same as the pre-selection region but with $\text{MET} > 50 \text{ GeV}$ and $60 < M_{T2}^H < 80 \text{ GeV}$.



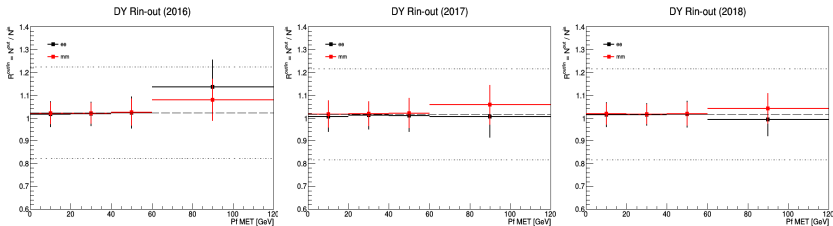
DY Rin-out method

We want to estimate the DY yields outside of the Z-peak from the data:

- Given the presence of large backgrounds (such as $t\bar{t}$) in the analysis region, we go inside of the Z-peak to compute the **Rin-out factor**:

$$N_{DY}^{out} = N_{DY, data}^{in} \cdot \kappa \cdot \left(\frac{N_{DY, MC}^{out}}{N_{DY, MC}^{in}} \right) \equiv N_{DY, data}^{in} \cdot \frac{R_{out/in, MC}^{0bj}}{R_{out/in, data}^{0bj}} \cdot R_{out/in, MC}$$

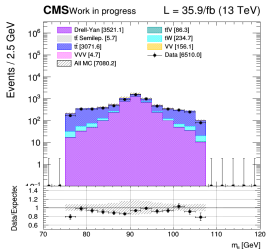
- To avoid any bias, the contamination of non-peaking backgrounds is removed and we correct this factor by the ratio κ between the data/MC transfer factors in a CR close to the SR (asking for 0 b-jet instead of 1);
- We then get this Rin-out in **bins of MET and for each channel ($ee, \mu\mu$) separately**:



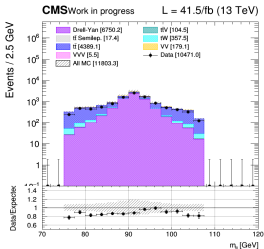
A flat scale factor and a fixed 20% systematic uncertainty is then applied to the DY. This

DY control region

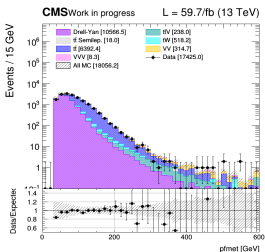
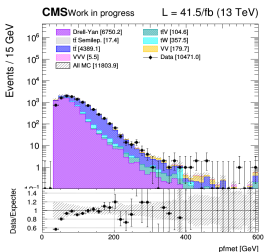
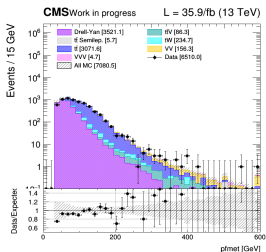
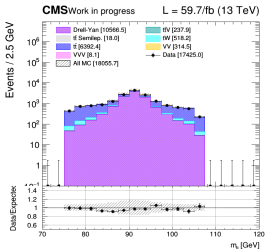
2016



2017



2018



The 0-bjet correction allows us to fix the data/MC discrepancies observed. A large systematic uncertainty is associated to this background, minor in the signal regions.

Systematic uncertainties

Systematic uncertainties

Most of the systematics to be considered (on top of the statistical uncertainties) are already in place, such as:

Theoretical uncertainties

- PDF and higher order corrections, underlying event and parton shower modeling, renormalization and factorization scales.

Experimental uncertainties

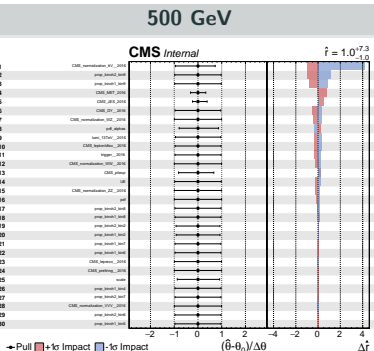
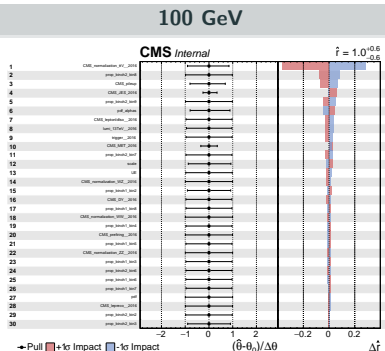
- Luminosity, pileup modeling, lepton trigger, lepton efficiency and energy scale, jet energy scale, MET mismodelling, b-tagging efficiency, top p_T reweighting, ECAL prefiring.

Background specific uncertainties

- 20% systematic uncertainty associated to the DY process in order to cover for the non-flatness of the $R_{\text{in-out}}$ transfer factor;
- 30% uncertainty associated to the normalization of all the minor backgrounds, except for the ttV, for which a 50% systematic uncertainty is associated.

Pulls and impact plots

2016

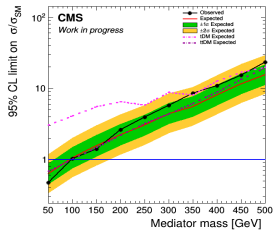


Results obtained

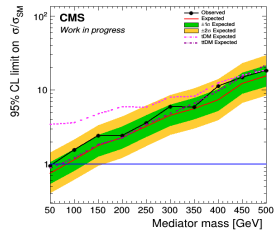
Upper limits

Scalar upper limits

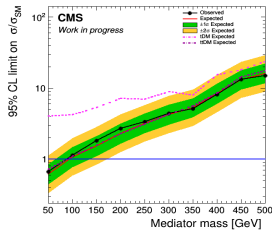
2016



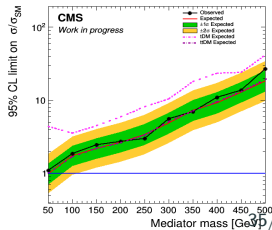
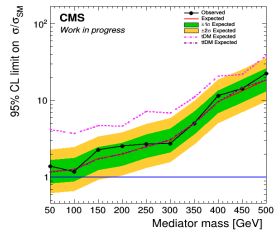
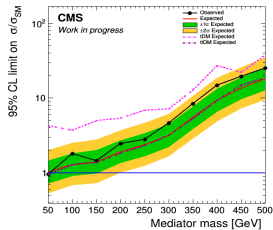
2017



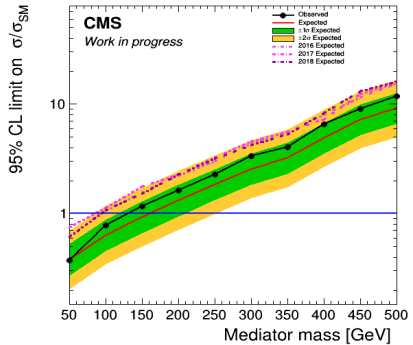
2018



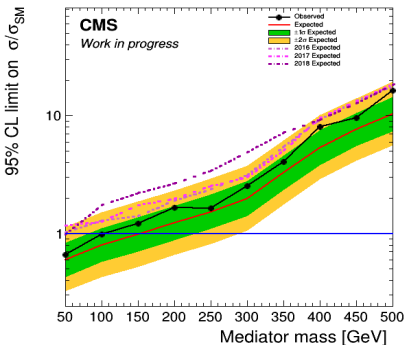
Pseudoscalar upper limits



Scalar mediators



Pseudoscalar mediators



After combination of the different years, an expected (observed) exclusion of:

- Scalar mediators is achieved up to 155 (130) GeV;
- Pseudoscalar mediators is obtained up to 150 (105) GeV.

Conclusions

A search for **dark matter produced in association with either one or two top quarks** has been performed, considering in particular its dilepton final state, and analyzing the **Run II legacy dataset** collected by the CMS detector at 13 TeV.

This is the **first time that such a combination of two signals of interest** is performed considering this final state.

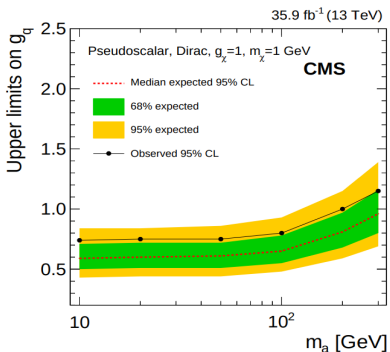
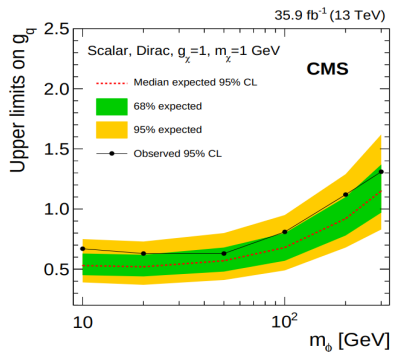
This search improves by a factor of 2 the scalar exclusion limits obtained in 2016 and manages to exclude for the first time pseudoscalar mediators up to 150 GeV.

We would therefore like to ask for the endorsement of the work performed here.

Back up

Additional relevant results

CMS combination of all the different final states published in 2016:



The observed (expected) limits excluded a **pseudoscalar mediator** with mass below 220 (320) GeV, and a **scalar mediator** with mass below 160 (240) GeV.

2016 data samples

| Dataset | Events (size) | \mathcal{L} [fb $^{-1}$] |
|--|---------------------|-----------------------------|
| Run 2016B | | |
| /DoubleEG/Run2016B_ver2-Nano02Apr2020_ver2-v1/NANOAOOD | 143073268 (99.4Gb) | |
| /DoubleMuon/Run2016B_ver2-Nano02Apr2020_ver2-v1/NANOAOOD | 82535526 (53.2Gb) | |
| /MuonEG/Run2016B_ver2-Nano02Apr2020_ver2-v1/NANOAOOD | 32727796 (26.8Gb) | 5.8 |
| /SingleElectron/Run2016B_ver2-Nano02Apr2020_ver2-v1/NANOAOOD | 246440440 (167.8Gb) | |
| /SingleMuon/Run2016B_ver2-Nano02Apr2020_ver2-v1/NANOAOOD | 158145722 (96.4Gb) | |
| Run 2016C | | |
| /DoubleEG/Run2016C-Nano02Apr2020-v1/NANOAOOD | 47677856 (35.3Gb) | |
| /DoubleMuon/Run2016C-Nano02Apr2020-v1/NANOAOOD | 27934629 (19.7Gb) | |
| /MuonEG/Run2016C-Nano02Apr2020-v1/NANOAOOD | 15405678 (12.8Gb) | 2.6 |
| /SingleElectron/Run2016C-Nano02Apr2020-v1/NANOAOOD | 97259854 (69.3Gb) | |
| /SingleMuon/Run2016C-Nano02Apr2020-v1/NANOAOOD | 67441308 (42.4Gb) | |
| Run 2016D | | |
| /DoubleEG/Run2016D-Nano02Apr2020-v1/NANOAOOD | 53324960 (39.6Gb) | |
| /DoubleMuon/Run2016D-Nano02Apr2020-v1/NANOAOOD | 33861745 (24.1Gb) | |
| /MuonEG/Run2016D-Nano02Apr2020-v1/NANOAOOD | 23482352 (19.4Gb) | 4.2 |
| /SingleElectron/Run2016D-Nano02Apr2020-v1/NANOAOOD | 148167727 (104.4Gb) | |
| /SingleMuon/Run2016D-Nano02Apr2020-v1/NANOAOOD | 98017996 (61.3Gb) | |
| Run 2016E | | |
| /DoubleEG/Run2016E-Nano02Apr2020-v1/NANOAOOD | 49877710 (37.9Gb) | |
| /DoubleMuon/Run2016E-Nano02Apr2020-v1/NANOAOOD | 28246946 (20.8Gb) | |
| /MuonEG/Run2016E-Nano02Apr2020-v2/NANOAOOD | 22519303 (19.0Gb) | 4.0 |
| /SingleElectron/Run2016E-Nano02Apr2020-v1/NANOAOOD | 117321545 (86.5Gb) | |
| /SingleMuon/Run2016E-Nano02Apr2020-v1/NANOAOOD | 90984718 (58.7Gb) | |
| Run 2016F | | |
| /DoubleEG/Run2016F-Nano02Apr2020-v1/NANOAOOD | 34577629 (26.9Gb) | |
| /DoubleMuon/Run2016F-Nano02Apr2020-v1/NANOAOOD | 20329921 (15.3Gb) | |
| /MuonEG/Run2016F-Nano02Apr2020-v1/NANOAOOD | 16002165 (13.6Gb) | 3.1 |
| /SingleElectron/Run2016F-Nano02Apr2020-v1/NANOAOOD | 70593532 (51.4Gb) | |
| /SingleMuon/Run2016F-Nano02Apr2020-v1/NANOAOOD | 65489554 (42.4Gb) | |
| Run 2016G | | |
| /DoubleEG/Run2016G-Nano02Apr2020-v1/NANOAOOD | 78797031 (61.6Gb) | |
| /DoubleMuon/Run2016G-Nano02Apr2020-v1/NANOAOOD | 45235604 (34.2Gb) | |
| /MuonEG/Run2016G-Nano02Apr2020-v1/NANOAOOD | 33854612 (29.0Gb) | 7.6 |
| /SingleElectron/Run2016G-Nano02Apr2020-v1/NANOAOOD | 153363109 (109.2Gb) | |
| /SingleMuon/Run2016G-Nano02Apr2020-v1/NANOAOOD | 149912248 (94.6Gb) | |
| Run 2016H | | |
| /DoubleEG/Run2016H-Nano02Apr2020-v1/NANOAOOD | 85388734 (67.7Gb) | |
| /DoubleMuon/Run2016H-Nano02Apr2020-v1/NANOAOOD | 48912812 (37.3Gb) | |
| /MuonEG/Run2016H-Nano02Apr2020-v1/NANOAOOD | 29236516 (26.0Gb) | 8.6 |
| /SingleElectron/Run2016H-Nano02Apr2020-v1/NANOAOOD | 128854598 (93.8Gb) | |
| /SingleMuon/Run2016H-Nano02Apr2020-v1/NANOAOOD | 174035164 (110.2Gb) | |

2017 data samples

| Dataset | Events (size) | $\mathcal{L} [\text{fb}^{-1}]$ |
|---|---------------------|--------------------------------|
| Run 2017B | | |
| /DoubleEG/Run2017B-Nano02Apr2020-v1/NANOAOD | 58088760 (46.6Gb) | |
| /DoubleMuon/Run2017B-Nano02Apr2020-v1/NANOAOD | 14501767 (10.8Gb) | |
| /SingleElectron/Run2017B-Nano02Apr2020-v1/NANOAOD | 60537490 (42.2Gb) | |
| /SingleMuon/Run2017B-Nano02Apr2020-v1/NANOAOD | 136300266 (86.2Gb) | |
| /MuonEG/Run2017B-Nano02Apr2020-v1/NANOAOD | 4453465 (4.1Gb) | |
| Run 2017C | | |
| /DoubleEG/Run2017C-Nano02Apr2020-v1/NANOAOD | 65181125 (53.8Gb) | |
| /DoubleMuon/Run2017C-Nano02Apr2020-v1/NANOAOD | 49636525 (39.5Gb) | |
| /SingleElectron/Run2017C-Nano02Apr2020-v1/NANOAOD | 136637888 (102.5Gb) | |
| /SingleMuon/Run2017C-Nano02Apr2020-v1/NANOAOD | 165652756 (109.5Gb) | |
| /MuonEG/Run2017C-Nano02Apr2020-v1/NANOAOD | 15595214 (15.0Gb) | |
| Run 2017D | | |
| /DoubleEG/Run2017D-Nano02Apr2020-v1/NANOAOD | 25911432 (21.6Gb) | |
| /DoubleMuon/Run2017D-Nano02Apr2020-v1/NANOAOD | 23075733 (18.6Gb) | |
| /SingleElectron/Run2017D-Nano02Apr2020-v1/NANOAOD | 51526710 (38.5Gb) | |
| /SingleMuon/Run2017D-Nano02Apr2020-v1/NANOAOD | 70361660 (47.2Gb) | |
| /MuonEG/Run2017D-Nano02Apr2020-v1/NANOAOD | 9164365 (8.9Gb) | |
| Run 2017E | | |
| /DoubleEG/Run2017E-Nano02Apr2020-v1/NANOAOD | 56233597 (49.8Gb) | |
| /DoubleMuon/Run2017E-Nano02Apr2020-v1/NANOAOD | 51589091 (44.4Gb) | |
| /SingleElectron/Run2017E-Nano02Apr2020-v1/NANOAOD | 102121689 (81.3Gb) | |
| /SingleMuon/Run2017E-Nano02Apr2020-v1/NANOAOD | 154630534 (111.0Gb) | |
| /MuonEG/Run2017E-Nano02Apr2020-v1/NANOAOD | 19043421 (19.2Gb) | |
| Run 2017F | | |
| /DoubleEG/Run2017F-Nano02Apr2020-v1/NANOAOD | 74307066 (67.1Gb) | |
| /DoubleMuon/Run2017F-Nano02Apr2020-v1/NANOAOD | 79756560 (68.0Gb) | |
| /SingleElectron/Run2017F-Nano02Apr2020-v1/NANOAOD | 128467223 (105.2Gb) | |
| /SingleMuon/Run2017F-Nano02Apr2020-v1/NANOAOD | 242135500 (178.3Gb) | |
| /MuonEG/Run2017F-Nano02Apr2020-v1/NANOAOD | 25776363 (26.3Gb) | |

2018 data samples

| Dataset | Events (size) | \mathcal{L} [fb^{-1}] |
|---|---------------------|------------------------------------|
| Run 2018A | | |
| /DoubleMuon/Run2018A-Nano02Apr2020-v1/NANO AOD | 75499908 (62.6Gb) | |
| /EGamma/Run2018A-Nano02Apr2020-v1/NANO AOD | 327843843 (261.8Gb) | |
| /SingleMuon/Run2018A-Nano02Apr2020-v1/NANO AOD | 241608232 (167.7Gb) | 13.5 |
| /MuonEG/Run2018A-Nano02Apr2020-v1/NANO AOD | 32958503 (32.3Gb) | |
| Run 2018B | | |
| /DoubleMuon/Run2018B-Nano02Apr2020-v1/NANO AOD | 35057758 (28.3Gb) | |
| /EGamma/Run2018B-Nano02Apr2020-v1/NANO AOD | 153822427 (123.1Gb) | |
| /SingleMuon/Run2018B-Nano02Apr2020-v1/NANO AOD | 119918017 (82.3Gb) | 6.8 |
| /MuonEG/Run2018B-Nano02Apr2020-v1/NANO AOD | 16211567 (15.8Gb) | |
| Run 2018C | | |
| /DoubleMuon/Run2018C-Nano02Apr2020-v1/NANO AOD | 34565869 (27.6Gb) | |
| /EGamma/Run2018C-Nano02Apr2020-v1/NANO AOD | 147827904 (119.2Gb) | |
| /SingleMuon/Run2018C-Nano02Apr2020-v1/NANO AOD | 110032072 (75.7Gb) | 6.6 |
| /MuonEG/Run2018C-Nano02Apr2020-v1/NANO AOD | 15652198 (15.3Gb) | |
| Run 2018D | | |
| /DoubleMuon/Run2018D-Nano02Apr2020_ver2-v1/NANO AOD | 168605834 (128.6Gb) | |
| /EGamma/Run2018D-Nano02Apr2020-v1/NANO AOD | 751348648 (583.6Gb) | |
| /SingleMuon/Run2018D-Nano02Apr2020-v1/NANO AOD | 513867253 (344.5Gb) | |
| /MuonEG/Run2018D-Nano02Apr2020_ver2-v1/NANO AOD | 71961587 (68.6Gb) | 32.0 |

2016 MC samples

| Process | Sample | Cross section [pb] |
|------------------|---|--------------------|
| Drell-Yan | DYJetsToLL_M-10to50_TuneCUETP8M1_13TeV-madgraphMLM-pythia8 | 18610.0 |
| | DYJetsToLL_M-50_TuneCUETP8M1_13TeV-madgraphMLM-pythia8 ($H_T < 70$ GeV) | 6077.22 |
| | DYJetsToLL_M-50_HT-70to100_TuneCUETP8M1_13TeV-madgraphMLM-pythia8 | 169.9 |
| | DYJetsToLL_M-50_HT-100to200_TuneCUETP8M1_13TeV-madgraphMLM-pythia8 | 147.4 |
| | DYJetsToLL_M-50_HT-200to400_TuneCUETP8M1_13TeV-madgraphMLM-pythia8 | 40.99 |
| | DYJetsToLL_M-50_HT-400to600_TuneCUETP8M1_13TeV-madgraphMLM-pythia8 | 5.678 |
| | DYJetsToLL_M-50_HT-600to800_TuneCUETP8M1_13TeV-madgraphMLM-pythia8 | 1.367 |
| | DYJetsToLL_M-50_HT-800to1200_TuneCUETP8M1_13TeV-madgraphMLM-pythia8 | 0.6304 |
| | DYJetsToLL_M-50_HT-1200to2500_TuneCUETP8M1_13TeV-madgraphMLM-pythia8 | 0.1514 |
| | DYJetsToLL_M-50_HT-2500toInf_TuneCUETP8M1_13TeV-madgraphMLM-pythia8 | 0.003565 |
| TTTo2L2Nu | TTTo2L2Nu_TuneCUETP8M2_ttHtranche3_13TeV-powheg-pythia8 | 87.310 |
| Single top | ST_s-channel_4f_leptonDecays_13TeV-amcatnlo-pythia8_TuneCUETP8M1 | 3.360 |
| | ST_t-channel_antitop_4f_inclusiveDecays_13TeV-powhegV2-madspin-pythia8_TuneCUETP8M1 | 80.95 |
| | ST_t-channel_top_4f_inclusiveDecays_13TeV-powhegV2-madspin-pythia8_TuneCUETP8M1 | 136.02 |
| | ST_tW_antitop_5f_inclusiveDecays_13TeV-powheg-pythia8_TuneCUETP8M1 | 35.85 |
| | ST_tW_top_5f_inclusiveDecays_13TeV-powheg-pythia8_TuneCUETP8M1 | 35.85 |
| TTToSemiLeptonic | TTToSemilepton_TuneCUETP8M2_ttHtranche3_13TeV-powheg-pythia8 | 364.35 |
| ttV | TTZToLLNuNu_M-10_TuneCP5_PSweights_13TeV-amcatnlo-pythia8 | 0.2814 |
| | TTZToQQ_TuneCUETP8M1_13TeV-amcatnlo-pythia8 | 0.5297 |
| | TTWJetsToLNu_TuneCUETP8M1_13TeV-amcatnloFXFX-madspin-pythia8 | 0.2043 |
| | TTWJetsToQQ_TuneCUETP8M1_13TeV-amcatnloFXFX-madspin-pythia8 | 0.4062 |
| VZ | WWTo2L2Nu_13TeV-powheg | 12.178 |
| | WZTo3LNu_TuneCUETP8M1_13TeV-powheg-pythia8 | 4.42965 |
| | WZTo2L2Q_13TeV_amcatnloFXFX_madspin_pythia8 | 5.595 |
| | ZZTo2L2Nu_13TeV_powheg_pythia8 | 0.5640 |
| | ZZTo2L2Q_13TeV_powheg_pythia8 | 3.22 |
| Others | WWWW_WWZ_WZZ_ZZZ_WWG | // |

2017 MC samples

| Process | Sample | Cross section [pb] |
|------------------|--|--------------------|
| Drell-Yan | DYJetsToLL_M-10to50_TuneCP5_13TeV-madgraphMLM-pythia8 | 18610 |
| | DYJetsToLL_M-50_TuneCP5_13TeV-madgraphMLM-pythia8 ($H_T < 70$ GeV) | 6077.22 |
| | DYJetsToLL_M-50_HT-70to100_TuneCP5_13TeV-madgraphMLM-pythia8 | 169.9 |
| | DYJetsToLL_M-50_HT-100to200_TuneCP5_13TeV-madgraphMLM-pythia8 | 147.4 |
| | DYJetsToLL_M-50_HT-200to400_TuneCP5_13TeV-madgraphMLM-pythia8 | 40.99 |
| | DYJetsToLL_M-50_HT-400to600_TuneCP5_13TeV-madgraphMLM-pythia8 | 5.678 |
| | DYJetsToLL_M-50_HT-600to800_TuneCP5_13TeV-madgraphMLM-pythia8 | 1.367 |
| | DYJetsToLL_M-50_HT-800to1200_TuneCP5_13TeV-madgraphMLM-pythia8 | 0.6304 |
| | DYJetsToLL_M-50_HT-1200to2500_TuneCP5_13TeV-madgraphMLM-pythia8 | 0.1514 |
| | DYJetsToLL_M-50_HT-2500toInf_TuneCP5_13TeV-madgraphMLM-pythia8 | 0.003565 |
| TTTo2L2Nu | TTTo2L2Nu_TuneCP5_13TeV-powheg-pythia8 | 87.310 |
| Single top | ST_s-channel_4f_leptonDecays_mtop1715_TuneCP5_PSweights_13TeV-amcatnlo-pythia8 | 3.360 |
| | ST_t-channel_antitop_4f_inclusiveDecays_TuneCP5_13TeV-powhegV2-madspin-pythia8 | 80.95 |
| | ST_t-channel_top_4f_inclusiveDecays_TuneCP5_13TeV-powhegV2-madspin-pythia8 | 136.02 |
| | ST_tW_antitop_5f_inclusiveDecays_TuneCP5_13TeV-powheg-pythia8 | 35.85 |
| | ST_tW_top_5f_inclusiveDecays_TuneCP5_13TeV-powheg-pythia8 | 35.85 |
| TTToSemiLeptonic | TTToSemiLeptonic_TuneCP5_13TeV-powheg-pythia8 | 364.35 |
| ttV | TTZToLLNuNu_M-10_TuneCP5_PSweights_13TeV-amcatnlo-pythia8 | 0.2814 |
| | TTZToQQ_TuneCUETP8M1_13TeV-amcatnlo-pythia8 | 0.5297 |
| | TTWJetsToLNu_TuneCP5_PSweights_13TeV-amcatnloFXFX-madspin-pythia8 | 0.2043 |
| | TTWJetsToQQ_TuneCUETP8M1_13TeV-amcatnloFXFX-madspin-pythia8 | 0.4062 |
| VZ | WWTo2L2Nu_NNPDF31_TuneCP5_PSweights_13TeV-powheg-pythia8 | 12.178 |
| | WZTo3LNu_TuneCUETP8M1_13TeV-powheg-pythia8 | 4.42965 |
| | WZTo2L2Q_13TeV_amcatnloFXFX_madspin_pythia8 | 5.595 |
| | ZZTo2L2Nu_13TeV_powheg_pythia8 | 0.5640 |
| | ZZTo2L2Q_13TeV_amcatnloFXFX_madspin_pythia8 | 3.22 |
| Others | WWW, WWZ, WZZ, ZZZ, WWG | // |

2018 MC samples

| Process | Sample | Cross section [pb] |
|------------------|--|--------------------|
| Drell-Yan | DYJetsToLL_M-10to50_TuneCP5_13TeV-madgraphMLM-pythia8 | 18610 |
| | DYJetsToLL_M-50_TuneCP5_13TeV-madgraphMLM-pythia8 ($H_T < 70$ GeV) | 6077.22 |
| | DYJetsToLL_M-50_HT-70to100_TuneCP5_PSweights_13TeV-madgraphMLM-pythia8 | 169.9 |
| | DYJetsToLL_M-50_HT-100to200_TuneCP5_13TeV-madgraphMLM-pythia8 | 147.4 |
| | DYJetsToLL_M-50_HT-200to400_TuneCP5_13TeV-madgraphMLM-pythia8 | 40.99 |
| | DYJetsToLL_M-50_HT-400to600_TuneCP5_13TeV-madgraphMLM-pythia8 | 5.678 |
| | DYJetsToLL_M-50_HT-600to800_TuneCP5_13TeV-madgraphMLM-pythia8 | 1.367 |
| | DYJetsToLL_M-50_HT-800to1200_TuneCP5_13TeV-madgraphMLM-pythia8 | 0.6304 |
| | DYJetsToLL_M-50_HT-1200to2500_TuneCP5_13TeV-madgraphMLM-pythia8 | 0.1514 |
| | DYJetsToLL_M-50_HT-2500toInf_TuneCP5_13TeV-madgraphMLM-pythia8 | 0.003565 |
| TTTo2L2Nu | TTTo2L2Nu_TuneCP5_13TeV-powheg-pythia8 | 87.310 |
| Single top | ST_s-channel_4f_leptonDecays_TuneCP5_13TeV-madgraph-pythia8 | 3.360 |
| | ST_t-channel_antitop_4f_InclusiveDecays_TuneCP5_13TeV-powheg-madspin-pythia8 | 80.95 |
| | ST_t-channel_top_4f_InclusiveDecays_TuneCP5_13TeV-powheg-madspin-pythia8 | 136.02 |
| | ST_tW_antitop_5f_inclusiveDecays_TuneCP5_13TeV-powheg-pythia8 | 35.85 |
| | ST_tW_top_5f_inclusiveDecays_TuneCP5_13TeV-powheg-pythia8 | 35.85 |
| TTToSemiLeptonic | TTToSemiLeptonic_TuneCP5_13TeV-powheg-pythia8 | 364.35 |
| ttV | TTZToLLNuNu_M-10_TuneCP5_PSweights_13TeV-amcatnlo-pythia8 | 0.2814 |
| | TTZToQQ_TuneCUETP8M1_13TeV-amcatnlo-pythia8 | 0.5297 |
| | TTWJetsToLNu_TuneCP5_PSweights_13TeV-amcatnloFXFX-madspin-pythia8 | 0.2043 |
| | TTWJetsToQQ_TuneCUETP8M1_13TeV-amcatnloFXFX-madspin-pythia8 | 0.4062 |
| VZ | WWTo2L2Nu_NNPDF31_TuneCP5_13TeV-powheg-pythia8 | 12.178 |
| | WZTo3LNu_TuneCP5_13TeV-amcatnloFXFX-pythia8 | 4.42965 |
| | WZTo2L2Q_13TeV_amcatnloFXFX_madspin_pythia8 | 5.595 |
| | ZZTo2L2Nu_TuneCP5_13TeV_powheg_pythia8 | 0.5640 |
| | ZZTo2L2Q_13TeV_amcatnloFXFX_madspin_pythia8 | 3.22 |
| Others | WWW, WWZ, WZZ, ZZZ, WWG | // |

| Mass point | Cross-section [pb] |
|---|-----------------------|
| Scalar mediators | |
| DMscalar_Dilepton_top_tWChan_Mchi1_Mphi10 | $4.959 \cdot 10^{-2}$ |
| DMscalar_Dilepton_top_tWChan_Mchi1_Mphi20 | $3.235 \cdot 10^{-2}$ |
| DMscalar_Dilepton_top_tWChan_Mchi1_Mphi50 | $1.323 \cdot 10^{-2}$ |
| DMscalar_Dilepton_top_tWChan_Mchi1_Mphi100 | $5.633 \cdot 10^{-3}$ |
| DMscalar_Dilepton_top_tWChan_Mchi1_Mphi150 | $3.397 \cdot 10^{-3}$ |
| DMscalar_Dilepton_top_tWChan_Mchi1_Mphi200 | $2.359 \cdot 10^{-3}$ |
| DMscalar_Dilepton_top_tWChan_Mchi1_Mphi250 | $1.720 \cdot 10^{-3}$ |
| DMscalar_Dilepton_top_tWChan_Mchi1_Mphi300 | $1.328 \cdot 10^{-3}$ |
| DMscalar_Dilepton_top_tWChan_Mchi1_Mphi350 | $1.018 \cdot 10^{-3}$ |
| DMscalar_Dilepton_top_tWChan_Mchi1_Mphi400 | $6.717 \cdot 10^{-4}$ |
| DMscalar_Dilepton_top_tWChan_Mchi1_Mphi450 | $4.535 \cdot 10^{-4}$ |
| DMscalar_Dilepton_top_tWChan_Mchi1_Mphi500 | $3.206 \cdot 10^{-4}$ |
| DMscalar_Dilepton_top_tWChan_Mchi1_Mphi1000 | $3.045 \cdot 10^{-5}$ |
| Pseudoscalar mediators | |
| DMpseudoscalar_Dilepton_top_tWChan_Mchi1_Mphi10 | $6.151 \cdot 10^{-3}$ |
| DMpseudoscalar_Dilepton_top_tWChan_Mchi1_Mphi20 | $5.869 \cdot 10^{-3}$ |
| DMpseudoscalar_Dilepton_top_tWChan_Mchi1_Mphi50 | $4.946 \cdot 10^{-3}$ |
| DMpseudoscalar_Dilepton_top_tWChan_Mchi1_Mphi100 | $3.658 \cdot 10^{-3}$ |
| DMpseudoscalar_Dilepton_top_tWChan_Mchi1_Mphi150 | $2.754 \cdot 10^{-3}$ |
| DMpseudoscalar_Dilepton_top_tWChan_Mchi1_Mphi200 | $2.097 \cdot 10^{-3}$ |
| DMpseudoscalar_Dilepton_top_tWChan_Mchi1_Mphi250 | $1.616 \cdot 10^{-3}$ |
| DMpseudoscalar_Dilepton_top_tWChan_Mchi1_Mphi300 | $1.253 \cdot 10^{-3}$ |
| DMpseudoscalar_Dilepton_top_tWChan_Mchi1_Mphi350 | $7.851 \cdot 10^{-4}$ |
| DMpseudoscalar_Dilepton_top_tWChan_Mchi1_Mphi400 | $4.371 \cdot 10^{-4}$ |
| DMpseudoscalar_Dilepton_top_tWChan_Mchi1_Mphi450 | $3.095 \cdot 10^{-4}$ |
| DMpseudoscalar_Dilepton_top_tWChan_Mchi1_Mphi500 | $2.321 \cdot 10^{-4}$ |
| DMpseudoscalar_Dilepton_top_tWChan_Mchi1_Mphi1000 | $2.791 \cdot 10^{-5}$ |

$t\bar{t} + \text{DM}$ signal samples

| Mass point | Cross-section [pb] |
|---|-----------------------|
| Scalar mediators | |
| TTbarDMJets.Dilepton.scalar._LO_TuneCP5_13TeV-madgraph-mcatnlo-pythia8.mChi_1.mPhi_50 | $3.405 \cdot 10^{-1}$ |
| TTbarDMJets.Dilepton.scalar._LO_TuneCP5_13TeV-madgraph-mcatnlo-pythia8.mChi_1.mPhi_100 | $8.027 \cdot 10^{-2}$ |
| TTbarDMJets.Dilepton.scalar._LO_TuneCP5_13TeV-madgraph-mcatnlo-pythia8.mChi_1.mPhi_150 | $2.673 \cdot 10^{-2}$ |
| TTbarDMJets.Dilepton.scalar._LO_TuneCP5_13TeV-madgraph-mcatnlo-pythia8.mChi_1.mPhi_200 | $1.158 \cdot 10^{-2}$ |
| TTbarDMJets.Dilepton.scalar._LO_TuneCP5_13TeV-madgraph-mcatnlo-pythia8.mChi_1.mPhi_250 | $6.020 \cdot 10^{-3}$ |
| TTbarDMJets.Dilepton.scalar._LO_TuneCP5_13TeV-madgraph-mcatnlo-pythia8.mChi_1.mPhi_300 | $3.579 \cdot 10^{-3}$ |
| TTbarDMJets.Dilepton.scalar._LO_TuneCP5_13TeV-madgraph-mcatnlo-pythia8.mChi_1.mPhi_350 | $2.376 \cdot 10^{-3}$ |
| TTbarDMJets.Dilepton.scalar._LO_TuneCP5_13TeV-madgraph-mcatnlo-pythia8.mChi_1.mPhi_400 | $1.443 \cdot 10^{-3}$ |
| TTbarDMJets.Dilepton.scalar._LO_TuneCP5_13TeV-madgraph-mcatnlo-pythia8.mChi_1.mPhi_450 | $9.025 \cdot 10^{-4}$ |
| TTbarDMJets.Dilepton.scalar._LO_TuneCP5_13TeV-madgraph-mcatnlo-pythia8.mChi_1.mPhi_500 | $6.204 \cdot 10^{-4}$ |
| TTbarDMJets.Dilepton.scalar._LO_TuneCP5_13TeV-madgraph-mcatnlo-pythia8.mChi_20.mPhi_100 | $7.993 \cdot 10^{-2}$ |
| TTbarDMJets.Dilepton.scalar._LO_TuneCP5_13TeV-madgraph-mcatnlo-pythia8.mChi_30.mPhi_100 | $8.052 \cdot 10^{-2}$ |
| TTbarDMJets.Dilepton.scalar._LO_TuneCP5_13TeV-madgraph-mcatnlo-pythia8.mChi_40.mPhi_100 | $8.147 \cdot 10^{-2}$ |
| TTbarDMJets.Dilepton.scalar._LO_TuneCP5_13TeV-madgraph-mcatnlo-pythia8.mChi_45.mPhi_100 | $8.319 \cdot 10^{-2}$ |
| TTbarDMJets.Dilepton.scalar._LO_TuneCP5_13TeV-madgraph-mcatnlo-pythia8.mChi_49.mPhi_100 | $8.304 \cdot 10^{-2}$ |
| TTbarDMJets.Dilepton.scalar._LO_TuneCP5_13TeV-madgraph-mcatnlo-pythia8.mChi_51.mPhi_100 | $9.735 \cdot 10^{-4}$ |
| TTbarDMJets.Dilepton.scalar._LO_TuneCP5_13TeV-madgraph-mcatnlo-pythia8.mChi_55.mPhi_100 | $4.835 \cdot 10^{-4}$ |
| Pseudoscalar mediators | |
| TTbarDMJets.Dilepton.pseudoscalar._LO_TuneCP5_13TeV-madgraph-mcatnlo-pythia8.mChi_1.mPhi_50 | $3.440 \cdot 10^{-2}$ |
| TTbarDMJets.Dilepton.pseudoscalar._LO_TuneCP5_13TeV-madgraph-mcatnlo-pythia8.mChi_1.mPhi_100 | $2.164 \cdot 10^{-2}$ |
| TTbarDMJets.Dilepton.pseudoscalar._LO_TuneCP5_13TeV-madgraph-mcatnlo-pythia8.mChi_1.mPhi_150 | $1.414 \cdot 10^{-2}$ |
| TTbarDMJets.Dilepton.pseudoscalar._LO_TuneCP5_13TeV-madgraph-mcatnlo-pythia8.mChi_1.mPhi_200 | $9.773 \cdot 10^{-3}$ |
| TTbarDMJets.Dilepton.pseudoscalar._LO_TuneCP5_13TeV-madgraph-mcatnlo-pythia8.mChi_1.mPhi_250 | $6.753 \cdot 10^{-3}$ |
| TTbarDMJets.Dilepton.pseudoscalar._LO_TuneCP5_13TeV-madgraph-mcatnlo-pythia8.mChi_1.mPhi_300 | $4.808 \cdot 10^{-3}$ |
| TTbarDMJets.Dilepton.pseudoscalar._LO_TuneCP5_13TeV-madgraph-mcatnlo-pythia8.mChi_1.mPhi_350 | $2.742 \cdot 10^{-3}$ |
| TTbarDMJets.Dilepton.pseudoscalar._LO_TuneCP5_13TeV-madgraph-mcatnlo-pythia8.mChi_1.mPhi_400 | $1.409 \cdot 10^{-3}$ |
| TTbarDMJets.Dilepton.pseudoscalar._LO_TuneCP5_13TeV-madgraph-mcatnlo-pythia8.mChi_1.mPhi_450 | $9.302 \cdot 10^{-4}$ |
| TTbarDMJets.Dilepton.pseudoscalar._LO_TuneCP5_13TeV-madgraph-mcatnlo-pythia8.mChi_1.mPhi_500 | $6.618 \cdot 10^{-4}$ |
| TTbarDMJets.Dilepton.pseudoscalar._LO_TuneCP5_13TeV-madgraph-mcatnlo-pythia8.mChi_20.mPhi_100 | $2.166 \cdot 10^{-2}$ |
| TTbarDMJets.Dilepton.pseudoscalar._LO_TuneCP5_13TeV-madgraph-mcatnlo-pythia8.mChi_30.mPhi_100 | $2.164 \cdot 10^{-2}$ |
| TTbarDMJets.Dilepton.pseudoscalar._LO_TuneCP5_13TeV-madgraph-mcatnlo-pythia8.mChi_40.mPhi_100 | $2.162 \cdot 10^{-2}$ |
| TTbarDMJets.Dilepton.pseudoscalar._LO_TuneCP5_13TeV-madgraph-mcatnlo-pythia8.mChi_45.mPhi_100 | $2.180 \cdot 10^{-2}$ |
| TTbarDMJets.Dilepton.pseudoscalar._LO_TuneCP5_13TeV-madgraph-mcatnlo-pythia8.mChi_49.mPhi_100 | $2.151 \cdot 10^{-2}$ |
| TTbarDMJets.Dilepton.pseudoscalar._LO_TuneCP5_13TeV-madgraph-mcatnlo-pythia8.mChi_51.mPhi_100 | $1.993 \cdot 10^{-3}$ |
| TTbarDMJets.Dilepton.pseudoscalar._LO_TuneCP5_13TeV-madgraph-mcatnlo-pythia8.mChi_55.mPhi_100 | $7.750 \cdot 10^{-4}$ |

2016 triggers

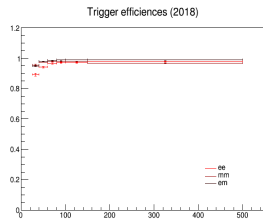
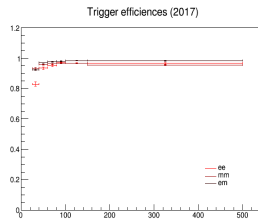
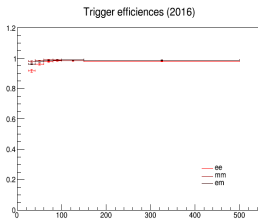
| Dataset | Run range | HLT trigger path |
|-----------|---|--|
| SingleMu | [297020,306462] | HLT_IsoMu27_v* |
| SingleEle | [297020,306462] | HLT_Ele35_WPTight_Gsf_v* |
| DoubleEG | [297020,306462] | HLT_Ele23_Ele12_CaloIdL_TrackIdL_IsoVL_v* |
| DoubleMu | [297020,299336] [299337,306462] | HLT_Mu17_TrkIsoVVL_Mu8_TrkIsoVVL_DZ_v* HLT_Mu17_TrkIsoVVL_Mu8_TrkIsoVVL_DZ_Mass8_v* |
| MuonEG | [297020,306462] [297020,299336] [299337,306462] | HLT_Mu12_TrkIsoVVL_Ele23_CaloIdL_TrackIdL_IsoVL_DZ_v* HLT_Mu23_TrkIsoVVL_Ele12_CaloIdL_TrackIdL_IsoVL_DZ_v* HLT_Mu23_TrkIsoVVL_Ele12_CaloIdL_TrackIdL_IsoVL_v* |

2017 triggers

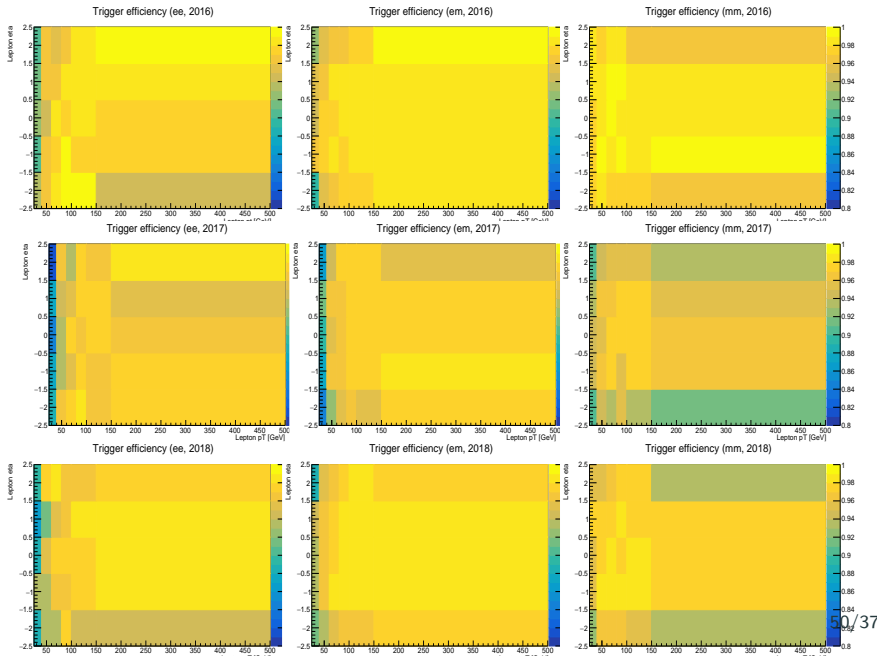
| Dataset | Run range | HLT trigger path |
|-----------|---|--|
| SingleMu | [297020,306462] | HLT_IsoMu27_v* |
| SingleEle | [297020,306462] | HLT_Ele35_WPTight_Gsf_v* |
| DoubleEG | [297020,306462] | HLT_Ele23_Ele12_CaloIdL_TrackIdL_IsoVL_v* |
| DoubleMu | [297020,299336] [299337,306462] | HLT_Mu17_TrkIsoVVL_Mu8_TrkIsoVVL_DZ_v* HLT_Mu17_TrkIsoVVL_Mu8_TrkIsoVVL_DZ_Mass8_v* |
| MuonEG | [297020,306462] [297020,299336] [299337,306462] | HLT_Mu12_TrkIsoVVL_Ele23_CaloIdL_TrackIdL_IsoVL_DZ_v* HLT_Mu23_TrkIsoVVL_Ele12_CaloIdL_TrackIdL_IsoVL_DZ_v* HLT_Mu23_TrkIsoVVL_Ele12_CaloIdL_TrackIdL_IsoVL_v* |

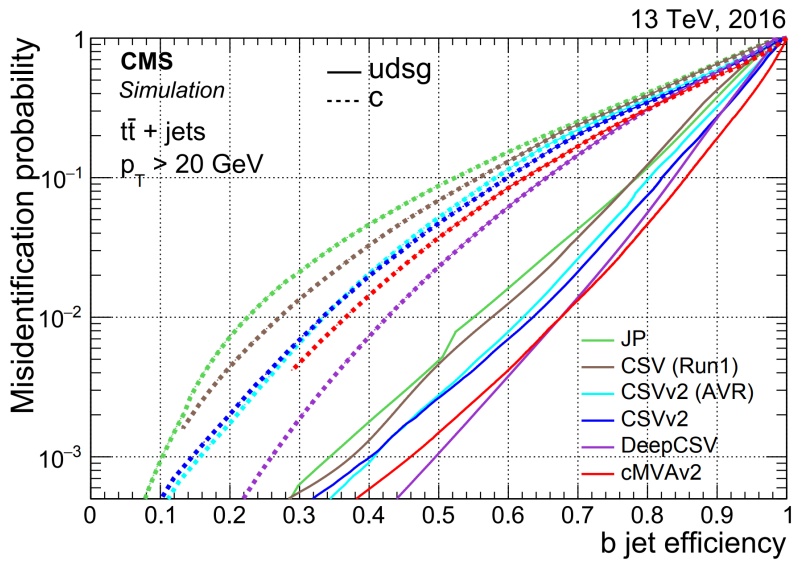
| Dataset | Run range | HLT trigger path |
|-----------|-----------------|---|
| SingleMu | [315252,325175] | HLT_IsoMu24_v* |
| SingleEle | [315252,325175] | HLT_Ele32_WPTight_Gsf_v* |
| DoubleEG | [315252,325175] | HLT_Ele23_Ele12_CaloIdL_TrackIdL_IsoVL_v* |
| DoubleMu | [315252,325175] | HLT_Mu17_TrkIsoVVL_Mu8_TrkIsoVVL_DZ_Mass3p8_v* |
| MuonEG | [315252,325175] | HLT_Mu23_TrkIsoVVL_Ele12_CaloIdL_TrackIdL_IsoVL_v* |
| | | HLT_Mu12_TrkIsoVVL_Ele23_CaloIdL_TrackIdL_IsoVL_DZ_v* |

Trigger efficiencies computed using orthogonal MET datasets.



2D trigger efficiencies





MET filters

| Filter name | Applied to data | Applied to simulation |
|---|-----------------|-----------------------|
| Flag_goodVertices | ✓ | ✓ |
| Flag_globalSuperTightHalo2016Filter | ✓ | ✓ |
| Flag_HBHENoiseFilter | ✓ | ✓ |
| Flag_HBHENoiselsoFilter | ✓ | ✓ |
| Flag_EcalDeadCellTriggerPrimitiveFilter | ✓ | ✓ |
| Flag_BadPFMuonFilter | ✓ | ✓ |
| Flag_ecalBadCalibFilterV2 [†] | ✓ | ✓ |

[†] applied only to 2017 and 2018.

m_{bl}^t variable

If a b-jet is produced in a top-quark decay, its invariant mass is bounded from above by $\sqrt{m_t^2 - m_W^2} = 153$ GeV. Events compatible with two semileptonic top-quark decays can then be selected or rejected by introducing the observable m_{bl}^t :

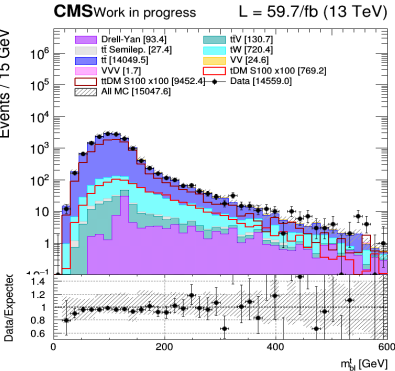
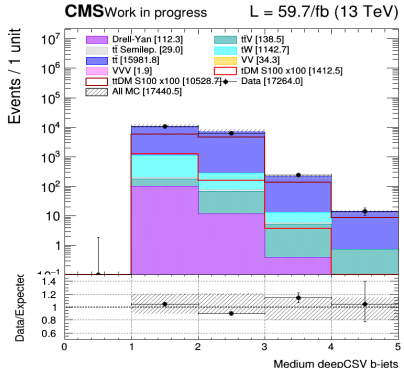
$$m_{bl}^t = \min (\max(m_{l_1 j_a}, m_{l_2 j_b}))$$

In this equation, the minimization is performed either:

- Over all the possible combinations of jets j_a, j_b among the b-jets of the events if three or more j-bets are observed;
- Or over the b-jet(s) observed plus the non b-tagged jet having the highest b-tag weight of the event.

This variable is expected to **give some discrimination** between our two signals of interest.

Number of b-jets and m_{bl}^t variable



Stransverse mass M_{T2}^{ll} and M_{T2}^{bl}

Extension of the transverse mass m_T to cases when pairs of same flavor particles decay into one visible and one invisible particle, such as the double $W \rightarrow l\nu$ decay.

Here, 2 neutrinos contribute to the presence of MET and the individual contribution of each particle ($\not{p}_{T_1}, \not{p}_{T_2}$) to this missing energy cannot be inferred. M_{T2}^{ll} is defined as:

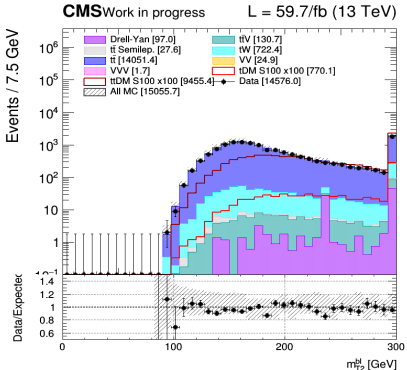
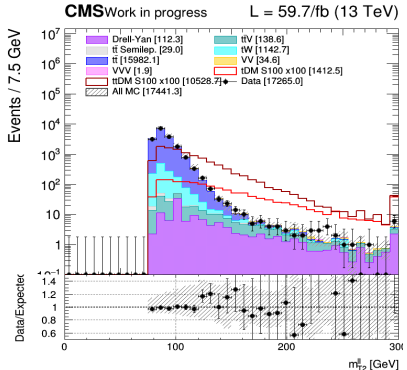
$$\begin{cases} M_{T2}^2 = \min_{\not{p}_{T_1} + \not{p}_{T_2} = \not{p}_{T_{\text{tot}}}} \left(\max \left(m_T^2(\not{p}_{T_1}, \not{p}_{T_1}), m_T^2(\not{p}_{T_2}, \not{p}_{T_2}) \right) \right) \\ m_T^2(\not{p}_T, \not{p}_T) = 4 |\not{p}_T| |\not{p}_T| \sin^2 \left(\frac{\alpha}{2} \right) \end{cases}$$

Different combinations $(\not{p}_{T_1}, \not{p}_{T_2})$ satisfying the condition $\not{p}_{T_1} + \not{p}_{T_2} = \not{p}_{T_{\text{tot}}}$ then need to be probed, keeping only the combination which results in the lowest possible value.

The $t\bar{t}$ process is expected to have an endpoint exactly at the mass of the W boson, while our eventual signal does not have this limitation because of the pair of dark matter particles produced.

The M_{T2}^{bl} variable is defined in a similar case, except that in this case, the lepton is paired with a b-jet. The jet/lepton permutation giving the smallest value is kept.

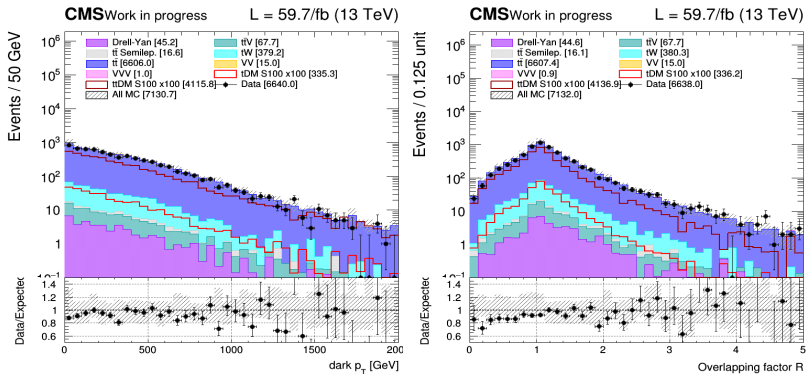
Transverse mass M_{T2}^{ll} and M_{T2}^{bl}



Dark p_T and overlapping factor R

Two discriminating variables naturally arise from the top reconstruction:

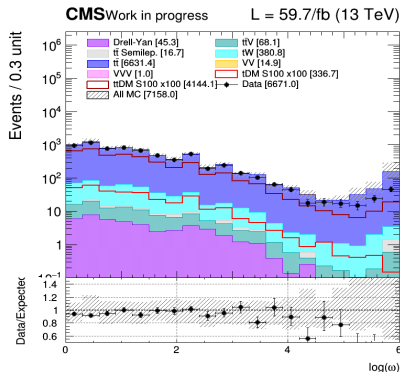
- The **dark p_T** , defined as the distance between the centroids of the ellipses;
- And the **overlapping factor R** , defined as the ratio between the size of the ellipses and the distance between them.



Top reconstruction weight W

The top reconstruction smearing process does introduce a new discriminating variable: the **top reconstruction weight W** .

Indeed, in order to know which lepton/b-jets combination and which smearing iteration performs the best, a weight is assigned to each iteration by comparing the invariant mass obtained m_{lb} with the expected distribution using generation. The combination with the largest weight is then simply considered as the solution of the event.

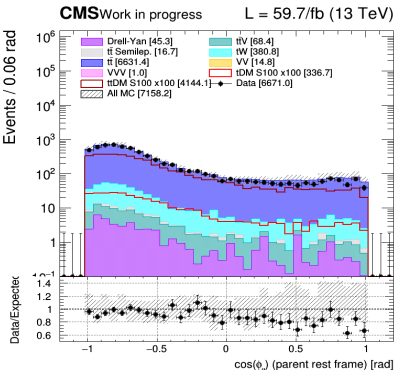
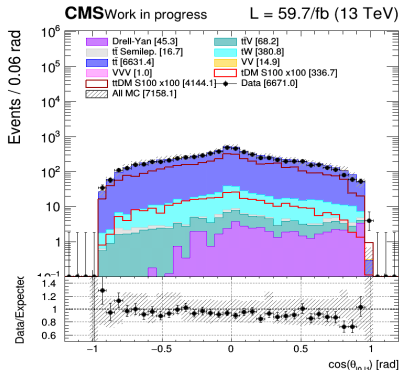


Spin correlated variables

The spin correlation in a $t\bar{t}$ -like event is expected to be conserved, because of the short lifetime of the top quark, and can be inferred from the top quark decay products.

Such variables are interesting because **the spin correlation depend on the production mechanism** and will be influenced by the additional coupling to a scalar or pseudoscalar mediator, making this a perfect candidate to be good discriminating variables:

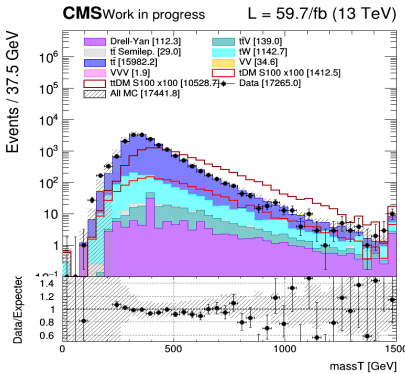
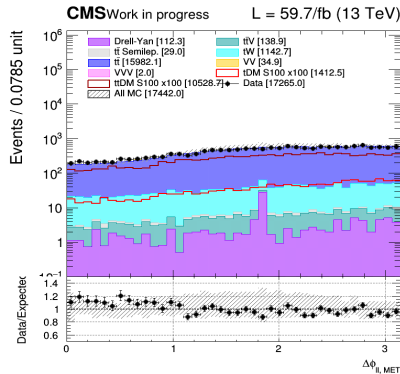
- $\xi = \cos(\theta_i) \cos(\theta_j)$, where i and j are either leptons, b-jets or neutrinos;
- $\cos(\Phi_{i,j})$, the cosine of the full opening angle of such top decay products in their respective parent rest frames.



Other discriminating variables I

Several other variables were considered for their discriminating power:

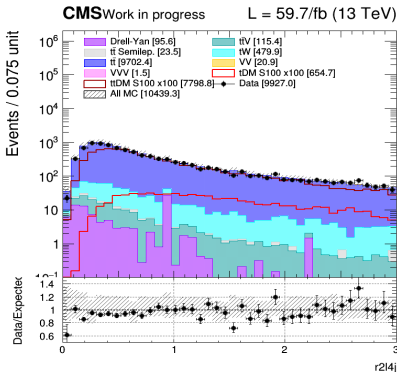
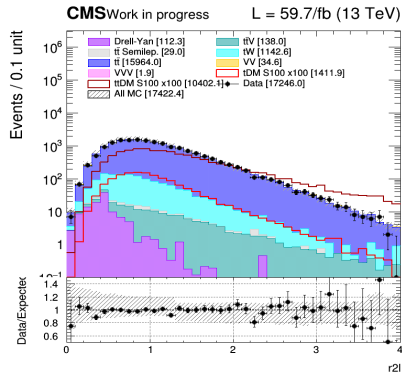
- $\Delta\Phi(E_T^{\text{miss}}, \text{II})$: the distribution in Φ of the two leptons is expected to change depending on the eventual production of DM;
- massT, which corresponds to the scalar sum of the transverse component of the MET, the two leptons and the two b-jets obtained by the top reconstruction process also helps with the discrimination process.



Other discriminating variables II

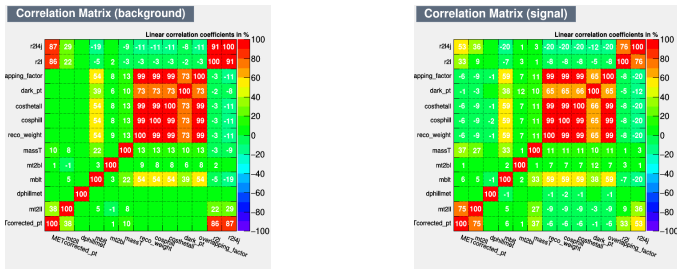
Two other interesting variables used by the ATLAS collaboration for their own analysis:

- $r2l$, defined as the ratio between the MET and the p_T of the two leptons observed;
- And $r2l4j$, defined in a similar way but considering additionally the p_T of the first 4 jets (if they exist) in the sum in the denominator.

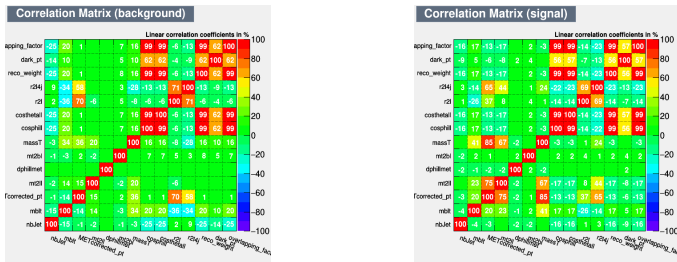


Input variables correlation

t/\bar{t} +DM region



$t\bar{t}$ +DM region

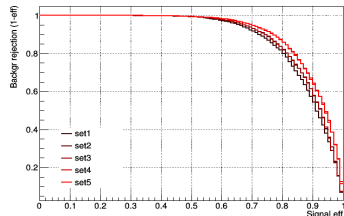


Input variables

BDT ROC curves

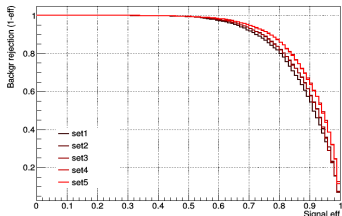
$t/\bar{t}+DM$ region

ROC curves for several trainings



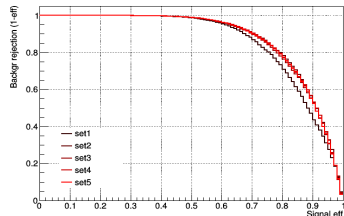
$t\bar{t}+DM$ region

ROC curves for several trainings

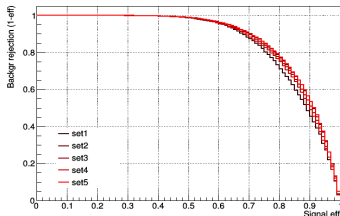


ANN ROC curves

ROC curves for several trainings



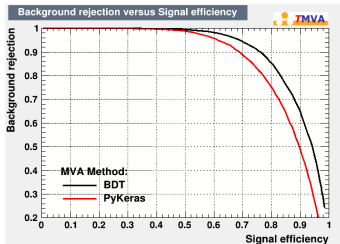
ROC curves for several trainings



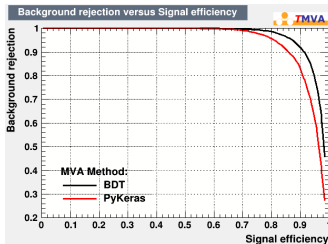
BDT vs ANN (t/\bar{t} +DM region)

Scalar mediators

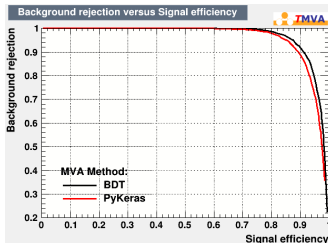
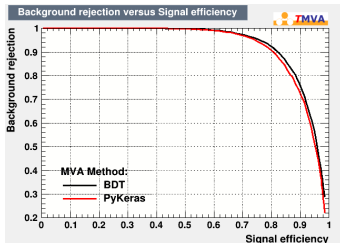
100 GeV



500 GeV



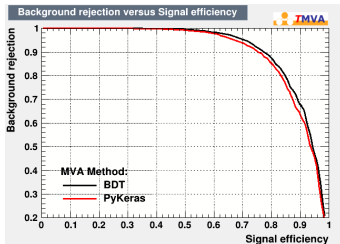
Pseudoscalar mediators



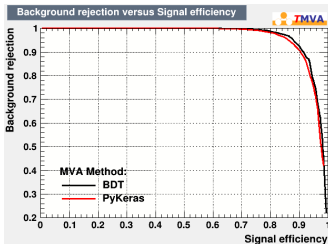
BDT vs ANN ($t\bar{t}$ +DM region)

Scalar mediators

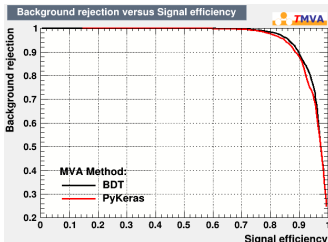
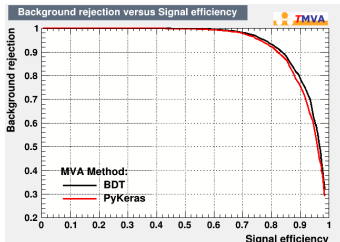
100 GeV



500 GeV



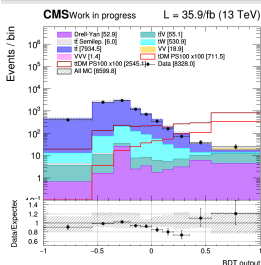
Pseudoscalar mediators



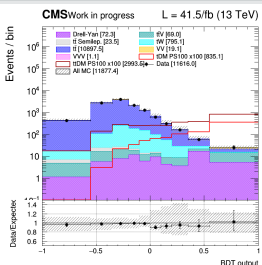
BDT pseudoscalar 100 GeV output shape

t/\bar{t} +DM region

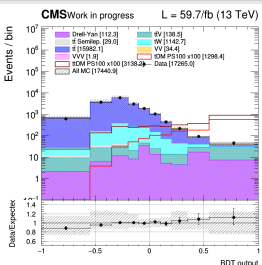
2016



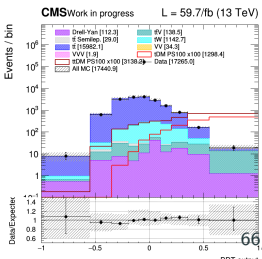
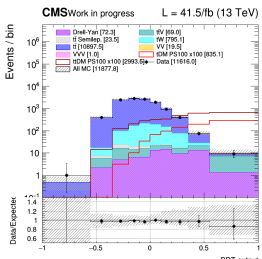
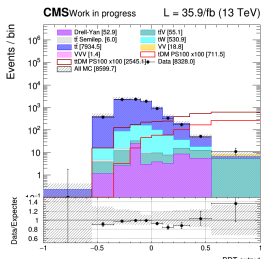
2017



2018



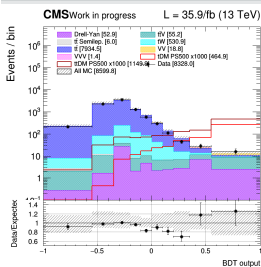
$t\bar{t}$ +DM region



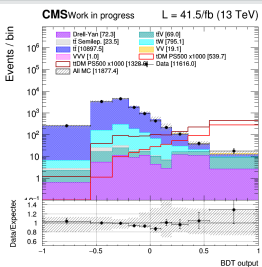
BDT pseudoscalar 500 GeV output shape

t/\bar{t} +DM region

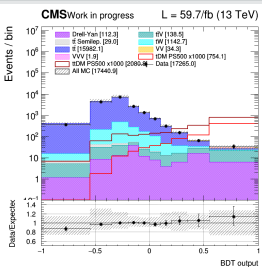
2016



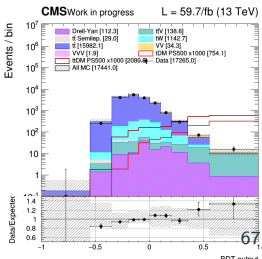
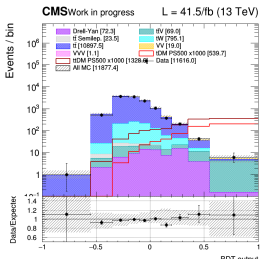
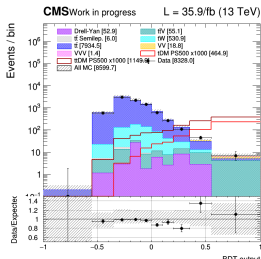
2017



2018



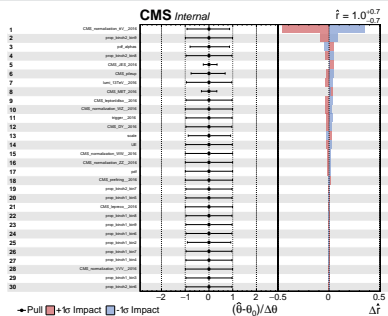
$t\bar{t}$ +DM region



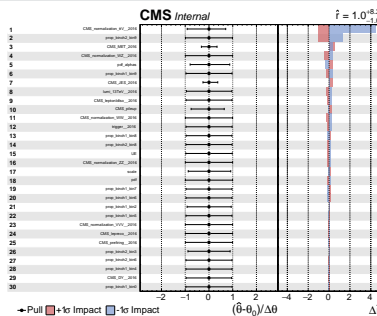
Pulls and impact plots

2016, pseudoscalar

100 GeV



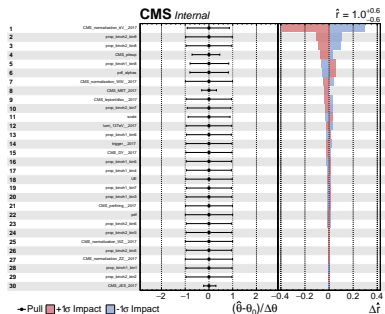
500 GeV



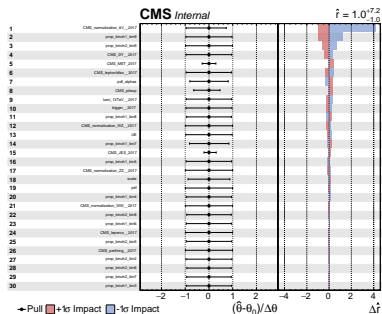
Pulls and impact plots

2017, scalar

100 GeV

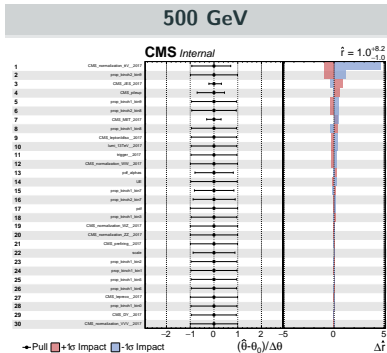
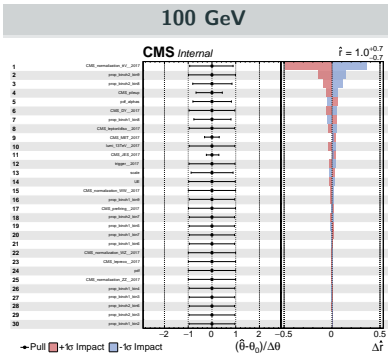


500 GeV



Pulls and impact plots

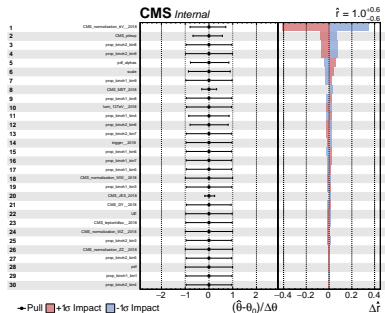
2017, pseudoscalar



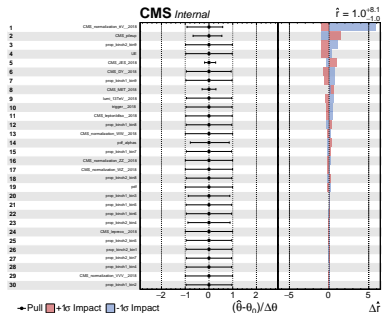
Pulls and impact plots

2018, scalar

100 GeV



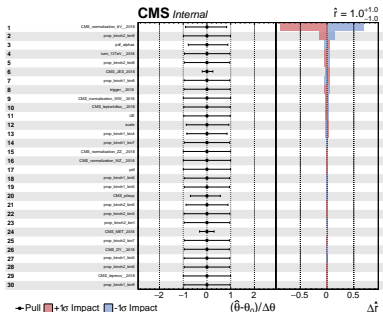
500 GeV



Pulls and impact plots

2018, pseudoscalar

100 GeV



500 GeV

